THE JOURNAL OF BIOLOGICAL CHEMISTRY VOL. 285, NO. 28, pp. 21736–21749, July 9, 2010

Valosin-containing Protein (VCP) in Novel Feedback Machinery between Abnormal Protein Accumulation and Transcriptional Suppression*[S]

Received for publication, December 29, 2009, and in revised form, March 31, 2010 Published, JBC Papers in Press, April 21, 2010, DOI 10.1074/jbc.M109.099283

Masaaki Koike[‡], Junpei Fukushi[‡], Yuzuru Ichinohe[‡], Naoki Higashimae[‡], Masahiko Fujishiro[‡], Chiyomi Sasaki[‡], Masahiro Yamaguchi[§], Toshiki Uchihara[¶], Saburo Yagishita[‖], Hiroshi Ohizumi[‡], Seiji Hori[‡], and Akira Kakizuka[‡1]

From the [‡]Laboratory of Functional Biology, Kyoto University Graduate School of Biostudies & Solution Oriented Research for Science and Technology (JST), Kyoto 606-8501, Japan, the [§]Department of Physiology, Graduate School of Medicine, The University of Tokyo, Tokyo 113-0033, Japan, the [¶]Department of Neurology, Tokyo Metropolitan Institute for Neuroscience, Tokyo 183-8526, Japan, and the [‖]Department of Pathology, Kanagawa Rehabilitation Center, Kanagawa 243-0121, Japan

Abnormal protein accumulation is often observed in human neurodegenerative disorders such as polyglutamine diseases and Parkinson disease. Genetic and biochemical analyses indicate that valosin-containing protein (VCP) is a crucial molecule in the pathogenesis of human neurodegenerative disorders. We report here that VCP was specifically modified in neuronal cells with abnormal protein accumulation; this modification caused the translocation of VCP into the nucleus. Modification-mimic forms of VCP induced transcriptional suppression with deacetylation of core histones, leading to cell atrophy and the decrease of *de novo* protein synthesis. Preventing VCP nuclear translocation in polyglutamine-expressing neuronal cells and *Drosophila* eyes mitigated neurite retraction and eye degenerations, respectively, concomitant with the recovery of core histone acetylation. This represents a novel feedback mechanism that regulates abnormal protein levels in the cytoplasm during physiological processes, as well as in pathological conditions such as abnormal protein accumulation in neurodegenerations.

Homeostasis is a fundamental property of organisms and cells that allows them to remain healthy in the face of changes in the environment. Feedback mechanisms are the core machinery for maintaining homeostasis. One example of feedback mechanism is end-product inhibition in enzyme reactions, and another is unfolded protein response (UPR)[2] in ER (1, 2). The goal of UPR is to reduce the amount of accumulated misfolded proteins in the ER (3). Although there have been a number of studies of the elegant feedback mechanisms employed for ER quality control, it is currently unknown whether similar mechanisms exist to reduce the cytoplasmic accumulation of misfolded proteins. Many neurodegenerative diseases (*e.g.* polyglutamine diseases, AD, PD, and ALS) share pathological features such as accumulation of abnormal proteins, neural cell atrophy, or degeneration, and neuronal cell death (4, 5), suggesting that common molecular mechanisms underlie these disorders. Indeed polyglutamine expansions have been identified in aggregated proteins in nine inherited neurodegenerative disorders, including HD and MJD (also called SCA3), α-synuclein in PD, DLB, and multisystem atrophy, and TDP-43 in certain types of front-temporal dementia, PD without Lewy bodies, and ALS (4–6). These proteins accumulate in the cytoplasm, the nucleus, or both, and have been proposed to trigger multiple cellular responses, such as cell death, proteasomal dysfunction, ER stress, and oxidative stress (7–11), as well as transcriptional dysregulation (12, 13).

Transcriptional regulation of gene expression is often accompanied by histone modifications, such as acetylation, phosphorylation, ubiquitination, and methylation (14, 15). Among these, acetylation of core histones (such as H3 and H4) reflects the open chromatin configuration that allows the transcriptional machinery to easily access target genes and thus promote transcription (14, 16). Several groups have reported that polyglutamine aggregates suppress cellular functions at the transcription level, and that this suppression is accompanied by decreased acetylation of core histones. It has been argued that sequestration of major HATs (*e.g.* CBP, PCAF, and TAFII130) underlies this transcriptional suppression (12, 13, 17–19). It is notable that decreased acetylation of core histones and transcriptional dysregulation has been observed not only in polyglutamine disease models, but also in PD, ALS, and AD models (20–22). Unlike polyglutamine disease models, sequestration of transcription factors has not been observed in the PD, ALS, and AD disease models, suggesting that an as-yet unknown mechanism may underlie transcriptional dysregulation in these disorders.

Valosin-containing protein (VCP) is a member of the AAA protein family. VCP has been proposed to function in a variety of physiological processes such as cell cycle regulation, mem-

* This work was supported in part by research grants from the Ministry of Education, Culture, Sports, Science, and Technology of Japan.

[S] The on-line version of this article (available at http://www.jbc.org) contains supplemental Figs. S1–S8.

[1] To whom correspondence should be addressed. Tel.: 81-75-753-7675; Fax: 81-75-753-7676; E-mail: kakizuka@lif.kyoto-u.ac.jp.

[2] The abbreviations used are: UPR, unfolded protein response; VCP, valosin-containing protein; ER, endoplasmic reticulum; AD, Alzheimer disease; PD, Parkinson disease; ALS, amyotrophic lateral sclerosis; HD, Huntington disease; MJD, Machado-Joseph disease; SCA, spinocerebellar ataxia; DLB, dementia with Lewy bodies; TDP, TAR DNA-binding protein; HAT, histone acetyltransferase; AAA, ATPase associated with various cellular activities; ERAD, ER-associated degradation; SOD, superoxide dismutase; IBMPFD, inclusion body myopathy with Paget disease of bone and frontotemporal dementia; GFP, green fluorescent protein; LC/MS/MS, liquid chromatography/tandem mass spectrometry; NLS, nuclear localization signal; NES, nuclear exclusion signal; NI, nuclear inclusion; EF, elongation factor; HA, hemagglutinin; CMV, cytomegalovirus.

brane fusion, ER-associated degradation (ERAD), and ubiquitin-mediated protein degradation (23, 24). We previously identified VCP as a binding partner of MJD proteins with expanded polyglutamine tracts (25). Furthermore, VCP has been shown to colocalize not only with polyglutamine aggregates, but also with Lewy bodies in PD and DLB, SOD1 aggregates in ALS, and dystrophic neurites in AD (25–28). Several lines of evidence have shown that VCP can mediate both aggregate formation and clearance, which is reminiscent of yeast Hsp104, another AAA protein (see references in 29). In addition, by genetic screening using *Drosophila* models of polyglutamine disease, we identified *ter94*, the *Drosophila* homolog of VCP, as a genetic modifier of eye degeneration phenotypes induced by expanded polyglutamine tracts (30). VCP has also been shown to be highly modified by S-thiolation, phosphorylation, and acetylation (31–34).

Recently, about a dozen missense mutations in the human *VCP* gene have been identified as causing inclusion body myopathy with Paget disease of bone and frontotemporal dementia (IBMPFD), an autosomal dominant inherited disease that affects multiple tissues, including muscle, bone, and the cerebral cortex (35–39). Although it is now known that VCP is critically involved in the pathogenesis of several types of human disorders, including neurodegeneration, the detailed molecular mechanisms mediated by VCP in neurodegenerative disorders remain to be elucidated.

EXPERIMENTAL PROCEDURES

Antibodies—Polyclonal antibodies against VCP were developed in our laboratory and described previously (25, 40). The anti-FLAG antibodies (M2 and M5) were obtained from Sigma; anti-actin antibody from Chemicon; anti-histone H3, H4, acetyl-histone H3 (for acetylated Lys-9 and Lys-14), and acetyl-histone H4 (for acetylated Lys-5) antibodies from Upstate Cell Signaling. Anti-GFP and anti-HA antibodies are from Nacalai and Roche, respectively.

Cell Cultures and Transfection—HEK293, NIH3T3, and MCF7 cells were maintained in Dulbecco's modified Eagle's medium (DMEM) (high glucose) with 10% fetal bovine serum. PC12 and its derivative cells were maintained on type 4 collagen-coated culture dishes in DMEM (low glucose) with 10% fetal bovine serum and 5% horse serum with or without 0.5 μg/ml tetracycline. PC12 cell lines expressing wild-type and mutant VCPs under the tet-off promoter were established following a standard procedure as described previously (40). S2R+ cells (41) were maintained in Schneider's *Drosophila* medium with 10% fetal bovine serum. When needed, cells were transfected with expression plasmids using Lipofectamine Plus, Lipofectamine 2000TM, or Cellfectin (Invitrogen).

Construction of Expression Vectors—The full-length VCP cDNAs were subcloned into the pEGFP-N3 vector. The cDNAs for VCP mutants, in which Ser-612 and Thr-613, and Lys-614 were replaced to Asp or Ala, Glu or Ala, and Gln or Ala, respectively, were generated using a site-directed mutagenesis kit (Stratagene). NLS- or NES-coding oligonucleotides were inserted in-frame between the start codon and VCP cording regions. To generate *Drosophila* cell expression vectors, VCP-GFP, FLAG-ter94, and HA-Q79 were subcloned into the pUAST vector. pHrD-Luc was a gift from Drs. Kanda and Mori and contains the human rRNA promoter region spanning −410 to +314 bp (42). pRrD-Luc was constructed by inserting the rat rRNA promoter region spanning −169 to +73, into pGL3-basic vector (Promega).

Quantification of Cultured Cells with Reduced Histone Acetylation—Intensities of immunostaining of acetylated histones were quantified using Image Pro Plus 5.1 software (Media Cybernetics). For each experiment, we evaluated at least 100 cells. When the intensity of the measured cell was more than 25% below the average of control cells, we estimated this cell as having reduced histone acetylation.

Quantification of Cells with Retracted Neurites—PC12 cells with retracted neurites were scored by counting GFP-positive cells in which the neurite lengths were shorter than the cell diameter. For each experiment, we evaluated 100–200 cells. In the figures, the mean values of duplicate experiments are presented, and error bars are included.

Immunocytochemical Analyses—Fixed cells were permeabilized with 0.5% Triton X-100 buffer (0.5% Triton X-100, 20 mM HEPES, 50 mM NaCl, 3 mM $MgCl_2$, and 0.3 M sucrose) for 10 min at room temperature and blocked with blocking buffer (0.1% bovine serum albumin and 0.1% skim milk in phosphate-buffered saline) for 1 h. Cells were then incubated overnight at 4 °C with primary antibodies. Subsequently, cells were treated with Alexa Fluor 488, 546, or 647 secondary antibodies (Invitrogen). DNA was counterstained with TOTO-3 (Invitrogen). Images were taken with a LSM510 confocal microscope (Zeiss).

LC/MS/MS Analyses—Mammalian cell lines such as HEK293T cells were transfected with an expression vector for FLAG-VCP with or without an expression vector for Q79-GFP. Then, FLAG-VCP was immunoprecipitated and was separated by SDS-PAGE. Next, the samples were excised from the gels and were treated with trypsin. The tryptic-digested peptides were analyzed by LC/MS/MS (Waters, 2795 separation module/Thermo Finnigan, LCQ Deca XP plus) (34).

[^{35}S]Methionine/Cysteine Metabolic Labeling—Differentiated PC12 cells were incubated for 30 min in methionine/cysteine-free medium, then labeled for 30 min with 25 μCi of [^{35}S]methionine/cysteine (37 TBq/mmol) (GE Healthcare) in methionine/cysteine-free medium supplemented with 50 ng/ml of NGF in the medium. Ten micrograms of protein from the lysate was subjected to trichloroacetic acid preparation. Incorporated radio counts were measured by a liquid scintillation counter.

Q64C Transgenic Mice—The Q79C mice that we had previously created could not be bred due to very severe ataxia (7), but we recently established new polyglutamine transgenic mice, which express an HA-tagged C-terminal portion of MJD protein with 64 glutamine repeats (Q64C) in Purkinje cells by using the *L7* gene. In one mouse, the transgene integrated into the X chromosome, and we referred to this mouse as Q64C mouse. Thus, the female transgenic mice showed very mild ataxia, probably due to lyonization, and were breedable. We could observe two types of Purkinje cells in female cerebellum: cells with atrophic morphologies that expressed Q64C, and cells with normal morphologies, which did not express Q64C.

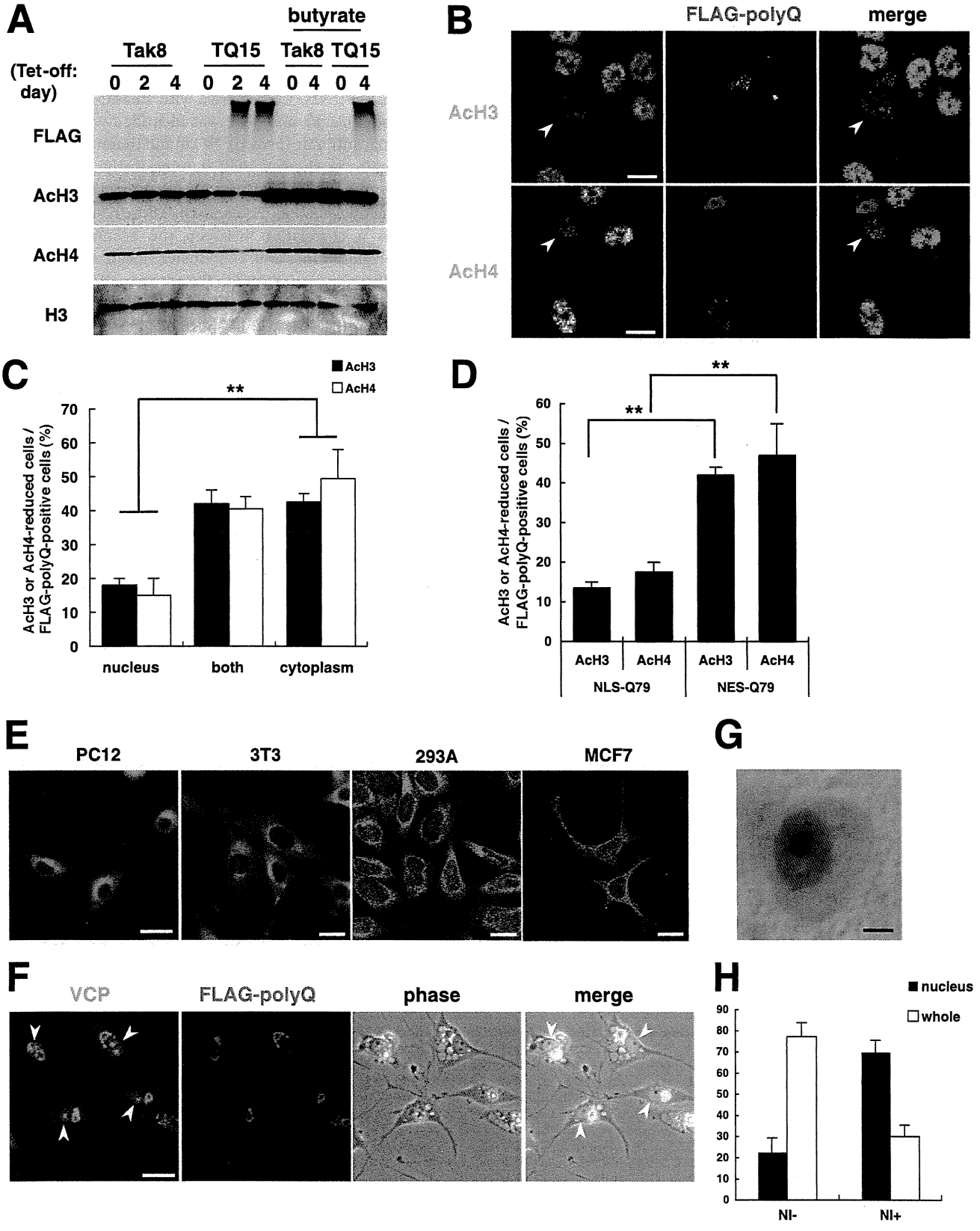

Transgenic Flies—Transgenic flies were created as described previously (30). Genotypes were the followings: GMR-Gal4/+ (+), GMR-Gal4/+; UAS-wtVCP/+ (wtVCP), GMR-Gal4/+; GMR-FlagQ92/+ (Q92), and GMR-Gal4/+; GMR-FlagQ92/ UAS-wtVCP (Q92/wtVCP).

Statistical Analysis—Each experiment was conducted at least three times with consistent results. The gel or blot representative of each experiment is presented. The statistical significance was analyzed using Student's *t* test.

RESULTS

Polyglutamine Aggregates, VCP Nuclear Translocation, and Histone Deacetylation—We had previously established a PC12 cell line (TQ15 cells) expressing FLAG-tagged 79-glutamine repeats (Q79) under the control of the tet-off promoter (40). Western blot analysis clearly demonstrated that Lys-9 and Lys-14 of H3 and Lys-5 of H4 were deacetylated after the expression of Q79 in a time-dependent manner (Fig. 1*A*). Addition of butyrate, an inhibitor of histone deacetylases, dramatically recovered or even enhanced the acetylation of histones H3 and H4, which was indistinguishable between cells with or without polyglutamine aggregates (Fig. 1*A* and supplemental Fig. S1). These observations fit well with the idea that expanded polyglutamine tracts contribute to enhancement of histone deacetylation rather than to diminishment of histone acetylation.

Surprisingly, significantly more cells with cytoplasmic aggregates showed a decrease in H3 and H4 acetylation than cells with nuclear aggregates alone (Fig. 1, *B* and *C*). We then transiently expressed NLS- or NES-tagged Q79 in parental PC12 cells and examined the location of aggregates and the acetylation levels of H3 and H4. As expected, all of the aggregates of NLS-Q79 or NES-Q79 were located in the nucleus or in the cytoplasm, respectively (data not shown). Significantly more cells expressing NES-Q79 showed a decrease in H3 and H4 acetylation than cells expressing NLS-Q79 (Fig. 1*D* and supplemental Fig. S2). This demonstrates that polyglutamine aggregates were able to induce core histone deacetylation, irrespective of whether they were nuclear or cytoplasmic.

We have long examined the relationship between VCP and the accumulation of abnormal proteins such as those containing expanded polyglutamines and noticed that VCP changes its localization from the cytoplasm to the nucleus even in cells with polyglutamine aggregates in the cytoplasm (Fig. 1, *E* and *F*), which was most often observed in neuronal cells. We then examined brain sections from our recently established Q64C mice and MJD patients. In Purkinje cells from normal mice, VCP was distributed diffusely throughout the cell. In contrast, VCP was mainly localized within the nucleus in the Q64C-expressing atrophic Purkinje cells of Q64C mice (supplemental Figs. S3 and S4). In the brain sections of MJD patients, nuclear inclusions (NIs) were stained with an anti-1C2 monoclonal antibody (black), and VCP was identified with an anti-VCP polyclonal antibody (brown). We found that nearly 80% of NI-positive neurons showed VCP staining in the nucleus. In contrast, only about 20% of NI-negative neurons showed VCP staining in the nucleus (Fig. 1, *G* and *H*). These results showed that there is a correlation between the accumulation of expanded polyglutamines and VCP nuclear localization.

VCP Modification and Atrophic Phenotypes—We have previously shown that VCP is highly modified by phosphorylation and acetylation (34). We thus purified FLAG-VCP from HEK293T cells expressing expanded polyglutamine tracts, analyzed it by LC/MS/MS, and found that three sequential amino acids, Ser-612, Thr-613, and Lys-614, were modified simultaneously by phosphorylation, phosphorylation, and acetylation, respectively (Fig. 2). These sequential modifications were not observed in VCP purified from cells expressing normal lengths of polyglutamines. The same sequential modifications were observed, although less frequently, in purified FLAG-VCP from MG132-treated cells (34). In the absence of MG132 treatment, these sequential modifications were not detected by LC/MS/MS analysis.

To elucidate the biological significance of these VCP modifications, we introduced amino acid substitutions mimicking these modifications into VCP. Ser-612, Thr-613, and Lys-614 were substituted with aspartic acid (D) (a negatively charged amino acid), glutamic acid (E) (another negatively charged amino acid), and glutamine (Q) (an uncharged amino acid), respectively, in various combinations. The resulting substituents were referred to as: VCP(**D**TK), VCP(S**E**K), and VCP(ST**Q**) (single substitutions); VCP(**DE**K) (double substitution); and VCP(**DEQ**) (triple substitution). In addition, alanine was introduced as several control substitutions. The resulting substituents were referred to as: VCP(AAK), VCP(AAQ), VCP(DEA), and VCP(AAA). These substituents, as well as wild-type VCP (wtVCP), were expressed as GFP-tagged proteins in PC12 cells. We were thus able to examine these exogenously expressed VCPs with live cell-imaging analysis as well as confocal imaging analysis. wtVCP was mainly localized in the cytoplasm. However, several modification-mimic VCPs

FIGURE 1. **Polyglutamine aggregates and histone deacetylation.** *A*, Western blot analysis of levels of FLAG-tagged Q79 (*FLAG*), acetylated histones H3 and H4 (*AcH3* and *AcH4*, respectively), and histone H3 (*H3*) before and 2 and 4 days after the removal of tetracycline from TQ 15 cells (*TQ15*) and parental PC12 cells (*Tak8*), in the absence and presence of 2.5 mM butyrate (*butyrate*). *B*, immunocytochemical analysis of acetylated histones H3 (*AcH3*) and H4 (*AcH4*) in PC12 cells transfected with FLAG-tagged Q79 (*FLAG-polyQ*) expression vector. Note that cells containing large polyglutamine aggregates (*arrowheads*) showed a clear decrease in acetylated histone levels. Merged images are shown in the *right panels* with indicated colors. *Bars*, 10 μm. *C*, quantification of immunocytochemical analysis in *B*. Cytoplasmic polyglutamine aggregates appeared to induce deacetylation of core histones (AcH3 and AcH4) in more cells than did nuclear polyglutamine aggregates. **, $p < 0.01$. *D*, quantification of immunocytochemical analyses of acetylated histones H3 (*AcH3*) and H4 (*AcH4*) in PC12 cells transfected with NLS-tagged FLAG-Q79 (*NLS-Q79*) or NES-tagged FLAG-Q79 (*NES-Q79*) expression vectors. **, $p < 0.01$. *E*, immunocytochemical analysis of endogenous VCP in PC12, NIH3T3 (*3T3*), HEK293A (*293A*), and MCF7 cells. VCP was stained with anti-VCP (*green*) and imaged by confocal microscopy. *Bars*, 20 μm. *F*, immunocytochemical analysis of endogenous VCP and FLAG-Q79 (*FLAG-polyQ*) in PC12 cells. VCP and FLAG-Q79 were stained with anti-VCP (*green*) and anti-FLAG (*red*), respectively, and imaged by confocal microscopy. PC12 cells with polyglutamine aggregates even in the cytoplasm showed clear VCP accumulation in the nucleus (*arrowheads*). *Bar*, 20 μm. *G*, immunohistochemical analysis of VCP in neurons from MJD patients. Brain sections from MJD patients were stained with anti-VCP (*brown*) and anti-1C2 for expanded polyglutamine (50) (*black*), and signals were visualized by the ABC method. *Bar*, 5 μm. *H*, quantification of VCP localization in the neurons from MJD patients in *G*. At least 200 neurons were imaged randomly and scored for localization of endogenous VCP in either nuclear inclusion-positive or -negative neurons.

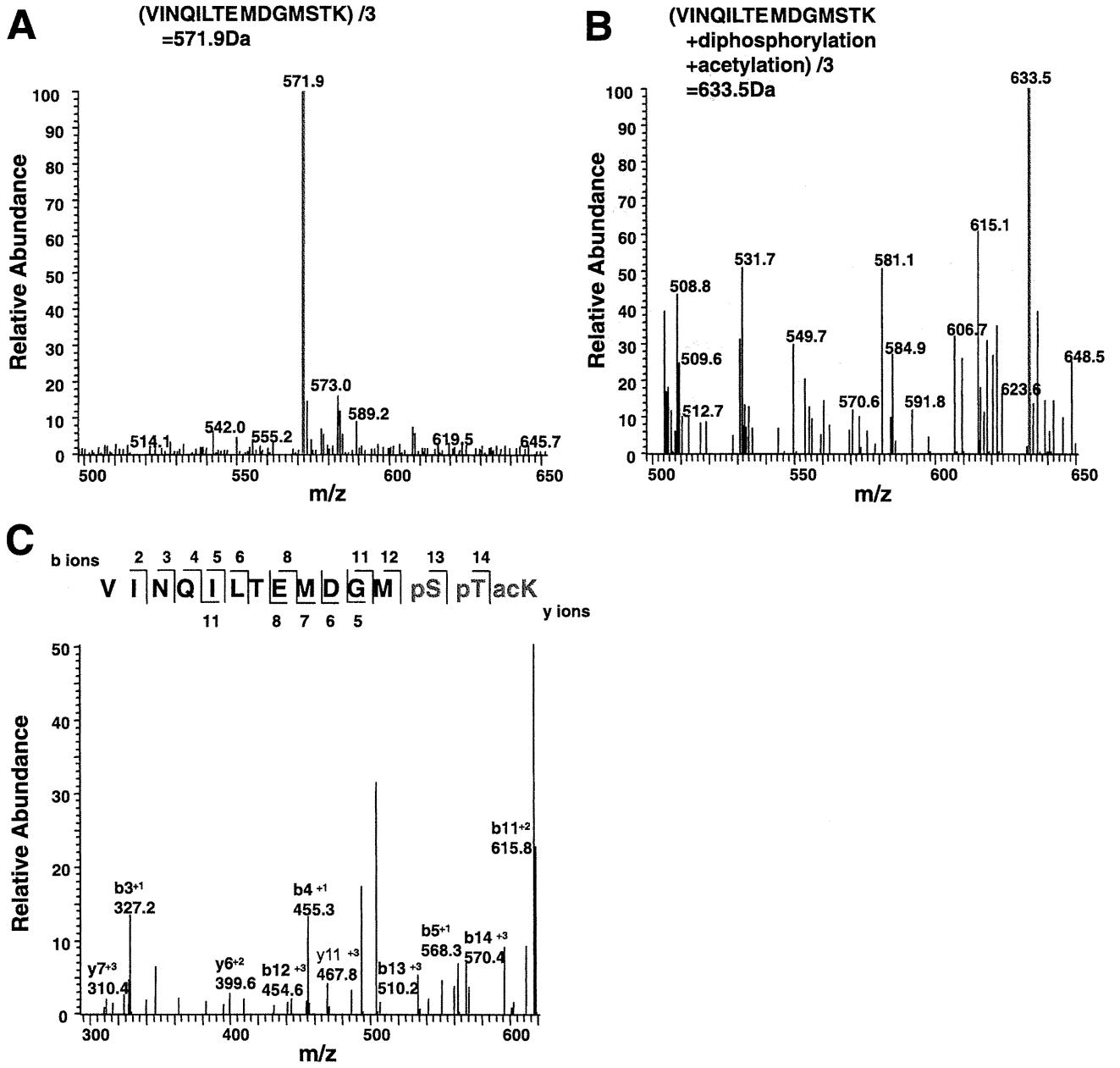

FIGURE 2. **Detection of modified Ser-612, Thr-613, and Lys-614 in VCP by LC/MS/MS analysis.** *A*, exclusive detection of the peptide from Val-600 to Lys-614 with molecular mass of 1,715.7 Da (571.9 Da ×3) in VCP recovered from non-treated HEK293T cells. From the molecular mass, two oxidized methionines were predicted, but any phosphorylation or acetylation site was not predicted in this peptide. *B*, detection of the modified peptide from Val-600 to Lys-614 with molecular mass of 1,900.5 Da (633.5 Da ×3) in VCP recovered from expanded polyglutamine-expressing HEK293T cells. From the molecular mass, one oxidized methionine, two phosphorylation sites, and one acetylation site were predicted in this peptide. *C*, an analytical data of LC/MS/MS with VCP recovered from expanded polyglutamine-expressing HEK293T cells. A tandem mass spectrum of the tryptic peptide with molecular mass of 1,900.5 Da (633.5 Da ×3) from immunoprecipitated FLAG-VCP shows detection of Ser-612, Thr-613, and Lys-614 being phosphorylated, phosphorylated, and acetylated, respectively. The MS/MS spectrum of the peptide with molecular mass of 633.5 Da ×3 in *B* was searched against a database constructed from the reported human VCP sequence utilizing SEQUEST program. Search parameters were modified to consider possible phosphorylation (+80) at all serine, threonine, or tyrosine residues, possible oxidation (+16) at methionine, and possible acetylation (+42) at lysine. Matched b or y ions via automatic computational interpretation are displayed as numbers in the sequence panel and the attribution of the strong peaks among them are indicated in the spectrum. Significant peaks that match to theoretical peaks interpreted by MS-Product are shown with numbers of the mass in the spectrum.

localized in the nucleus with different degrees. VCP(DEQ) was most often localized within the nucleus, followed by VCP(DEA) and VCP(DEK) (Fig. 3, *A* and *B*). VCP (AAA), VCP(AAQ), and VCP(AAK) were mostly excluded from the nucleus; less than 5% of transfected cells showed nuclear localization of these substituents (Fig. 3, *A* and *B*).

Surprisingly, 5 days after transfection, ~30% of the PC12 cells expressing VCP(DEQ) showed shrinkage of cell volume with neurite retraction (Fig. 3, *A* and *C*). We called this an "atrophic phenotype". The atrophic phenotype was most prominent in cells expressing VCP(DEQ), followed by VCP(DEA) and VCP(DEK) (Fig. 3*C*), and it was exactly correlated with

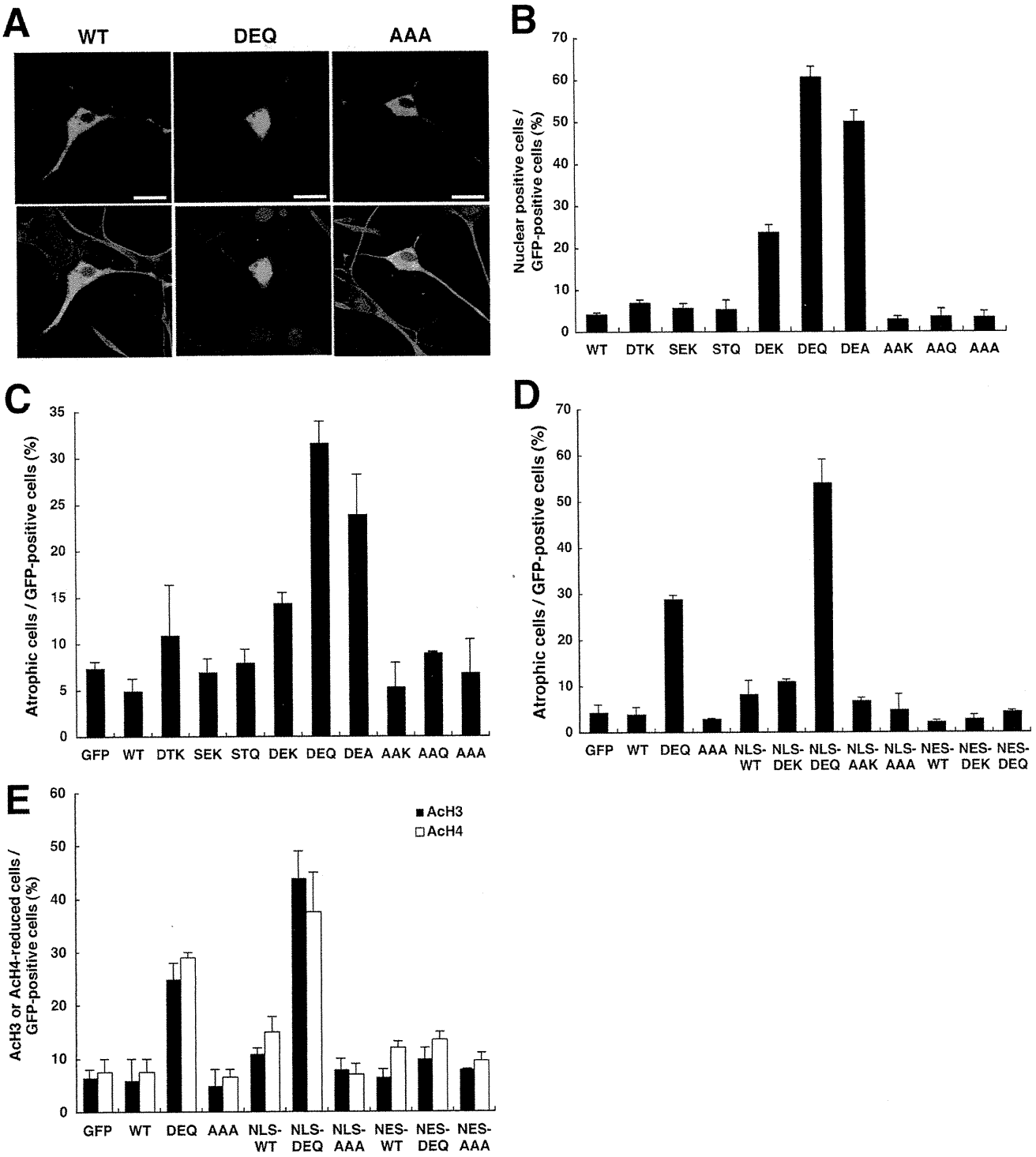

FIGURE 3. **Phenotypes of PC12 cells induced by modification-mimic forms of VCP.** *A*, immunocytochemical analysis of PC12 cells expressing GFP-tagged wild-type VCP, VCP(DEQ), and VCP(AAA). VCP(DEQ), but not wild-type VCP or VCP(AAA), localized within the nucleus. Four days after transfection, PC12 cells were fixed and stained with anti-GFP (*green*), anti-β-tubulin (*red*), and TOTO-3 (*blue*). PC12 cells expressing VCP(DEQ) showed retracted neurites and were small in size (atrophic phenotype). *Bars*, 20 μm. *B*, quantification of GFP-tagged wild-type and various forms of VCP localization in PC12 cells. At least 200 GFP-positive cells were imaged randomly and scored for the nuclear localization of GFP signals. *C*, quantification of atrophic phenotypes in PC12 cells expressing GFP-tagged wild-type and various forms of VCP. At least 200 GFP-positive cells were imaged randomly and scored for atrophic phenotypes. *D*, quantification of atrophic phenotypes in PC12 cells expressing GFP-tagged wild-type or various forms of VCP, some of which were also tagged with NLS or NES. At least 200 GFP-positive cells were imaged randomly and scored for atrophic phenotypes. *E*, quantification of immunocytochemical analysis for decreased histone acetylation in cells expressing GFP-tagged wild-type or various forms of VCP. At least 100 GFP-positive cells were imaged randomly and scored for decreased histone acetylation.

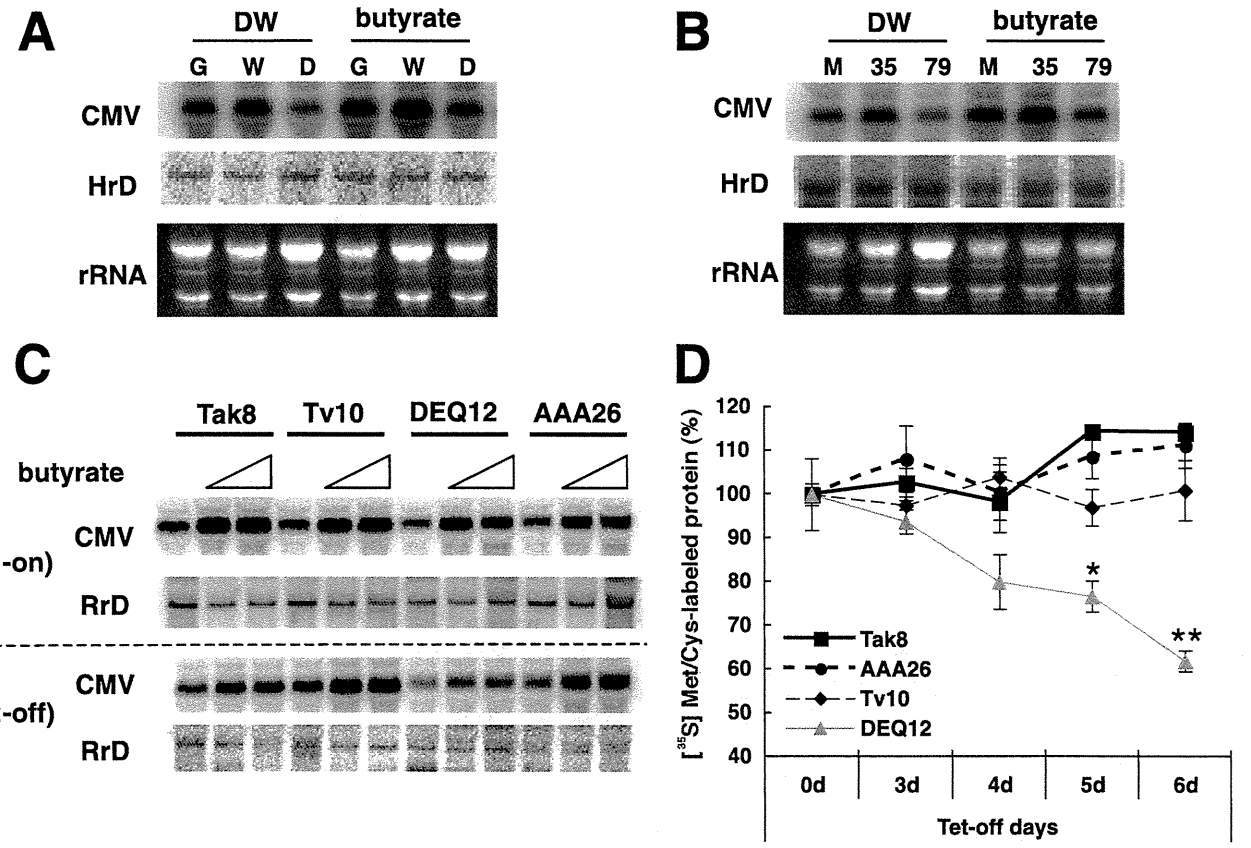

FIGURE 4. **VCP modification and suppression of transcription and protein synthesis.** *A*, Northern blot analysis of RNAs transcribed from CMV and human rRNA promoters in HEK293T cells. HEK293T cells were transfected with pCMV-luciferase 2 (*CMV*) and pHrRNA-luciferase (*HrD*), together with the expression vector for GFP (*G*), VCP-GFP (*W*), or VCP(DEQ)-GFP (*D*). Three days after transfection, RNAs were extracted and analyzed by Northern blot using radiolabeled luciferase or luciferase 2 cDNA as a probe. *B*, Northern blot analysis of RNAs transcribed from CMV and human rRNA promoters in HEK293T cells. HEK293T cells were transfected with pCMV-luciferase 2 (*CMV*) and pHrRNA-luciferase (*HrD*), together with an empty expression vector (*M*) or an expression vector for Q35 (*35*) or Q79 (*79*). Three days after transfection, RNAs were extracted and analyzed by Northern blot using radiolabeled luciferase or luciferase 2 cDNA as a probe. *C*, Northern blot analyses of RNAs transcribed from the CMV promoter in PC12 cells. Parental PC12 cells (Tak8) or PC12 cells expressing GFP-tagged wild-type VCP (Tv10), VCP(DEQ) (DEQ12), or VCP(AAA) (AAA26) under the control of the tet-off promoter were transfected with pCMV-luciferase 2 (*CMV*) together with pRrRNA-luciferase (*RrD*). One day after transfection, different amounts of butyrate (1 and 2.5 mM) were added in the presence (Tet-on) or absence (Tet-off) of tetracycline. Three days after transfection, RNAs were extracted and analyzed. The same blots were sequentially probed with radiolabeled luciferase 2 and luciferase cDNAs. *D*, measurement of *de novo* protein synthesis in Tak8, Tv10, DEQ12, and AAA26 cells. In the presence of tetracycline (0d) or 3, 4, 5, 6 days after it was removed, cells were labeled with [^{35}S]Met/Cys for 30 min and lysed. Incorporated radio counts were measured as described under "Experimental Procedures." Experiments were performed in duplicate, and mean values and error bars are presented. **, $p < 0.01$.

their nuclear translocation (Fig. 3, *B* and *C*). More cells expressing VCP(DEQ) showed an atrophic phenotype with increasing time, but remained alive even 7 days after transfection (data not shown). We could observe very little of the atrophic phenotype in cells expressing wtVCP (less than 5%).

We next sought to determine the cause of the atrophic phenotype, whether it was VCP nuclear localization, VCP amino acid substitution, or both. To this end, we expressed NLS- and NES-tagged wtVCP and several substituents in PC12 cells, and examined the phenotypes. All of the NLS-tagged VCPs translocated to the nucleus, and all of the NES-tagged VCPs stayed in the cytoplasm (data not shown). NLS-VCP(DEQ) induced the atrophic phenotype most frequently (more than 50% of cells) (Fig. 3*D*). The expression of other NLS-tagged VCPs (wtVCP, VCP(DEK), VCP(AAK), and VCP(AAA)) either did not result in or only marginally increased the atrophic phenotype (Fig. 3*D*). Conversely, NES-VCP(DEQ) did not result in the atrophic phenotype (Fig. 3*D*). These data demonstrate that both the modifications and the nuclear localization of VCP were necessary for the atrophic phenotype. Taken together, the above results suggested that modified VCP mediates a signal from the cytoplasm to the nucleus, leading to histone deacetylation. Indeed, deacetylations of H3 and H4 histones were observed in cells expressing VCP(DEQ) and NLS-VCP(DEQ), but not or only marginally in cells expressing wtVCP or VCP(AAA), even in the presence of NLS (Fig. 3*E* and supplemental Fig. S5).

VCP Modification and the Suppression of Transcription and Protein Synthesis—We next examined whether VCP(DEQ) expression could suppress steady-state mRNA levels in a transient transfection assay. For this experiment, we prepared an expression vector for luciferase RNA with the rat or human ribosomal RNA (rRNA) promoter (pRrD-Luc or pHrD-Luc, respectively), as an internal transfection control. Northern blot analysis revealed that luciferase RNA levels from both of the rRNA promoters were not affected by the addition of α-amanitin (an inhibitor of RNA polymerase II) or butyrate, or by wtVCP or VCP(DEQ) expression. However, the addition of actinomycin D (an inhibitor of RNA polymerase I) completely

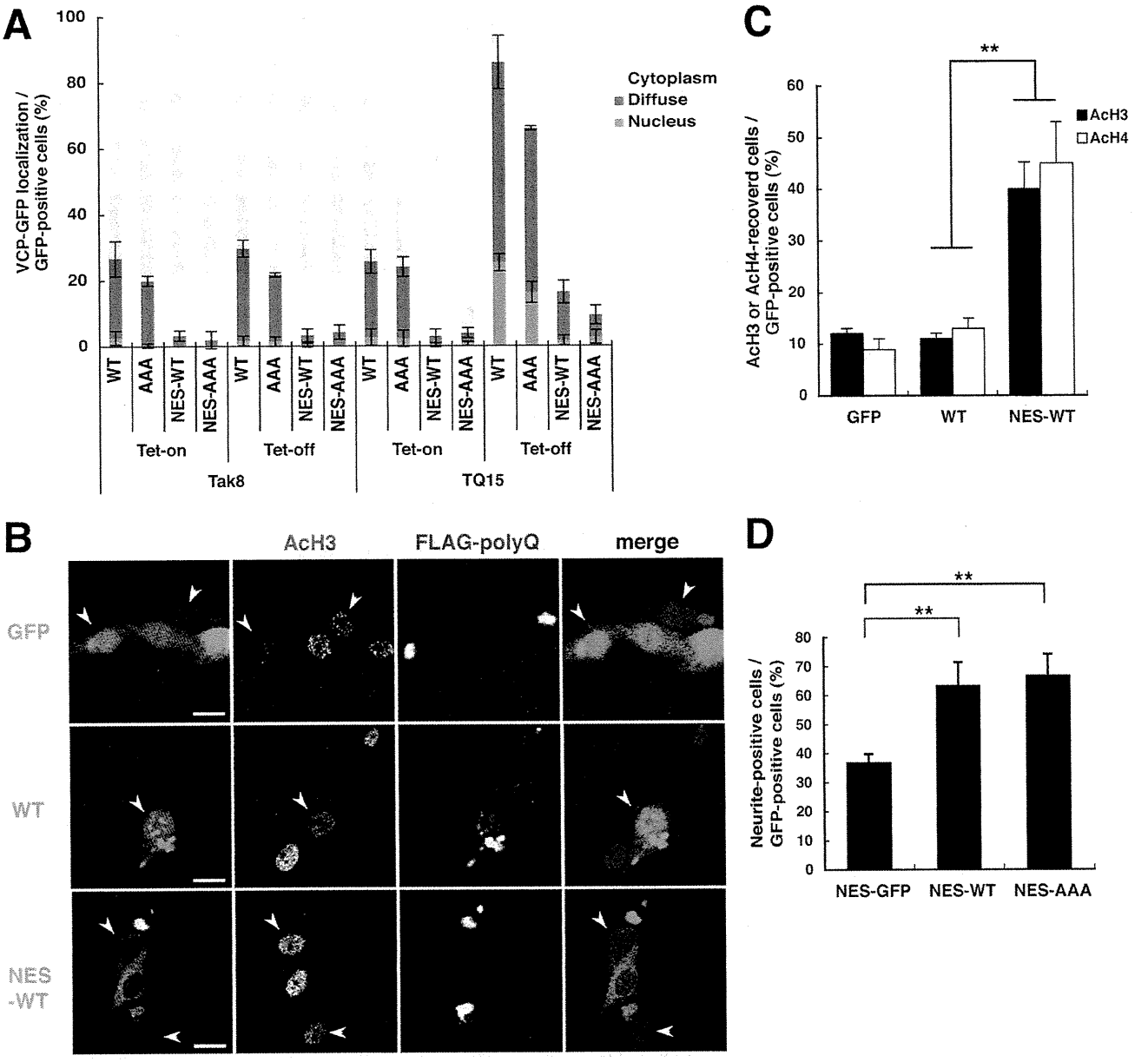

FIGURE 5. **Prevention of polyglutamine-induced histone deacetylation and neurite retraction by NES-VCPs.** *A*, quantification of intracellular localization of GFP-tagged wild-type or various forms of VCP in parental PC12 cells (Tak8) and PC12 cells expressing FLAG-Q79 under the control of the tet-off promoter (TQ15). TQ15 cells were transfected with GFP-tagged wild-type or various forms of VCP. One day after the transfection, tetracycline was removed from the media. Three days after removal of tetracycline, live cells were imaged for GFP signals. At least 200 GFP-positive cells were imaged randomly and scored. *B*, immunocytochemical analysis of TQ15 cells, transfected with GFP, GFP-tagged wild-type VCP (*WT*), or GFP- as well as NES-tagged wild-type VCP (*NES-WT*). One day after transfection, tetracycline was removed from the medium. Four days after removal of tetracycline, cells were fixed and stained with anti-GFP, anti-AcH3, and anti-FLAG. *Arrowheads*: cells containing polyglutamine aggregates. Merged images are also shown in the *right panels* with indicated colors. *Bars*, 15 μm. *C* and *D*, quantification of cells with recovered histone H3 acetylation levels (*C*) or neurite-positive cells (*D*) among GFP-positive PC12 cells expressing FLAG-Q79 under the same conditions as in *B*. At least 100 (*C*) and 200 (*D*) cells were imaged randomly and scored. **, $p < 0.01$.

blocked the luciferase RNA expression (Fig. 4, *A* and *B*, and supplemental Fig. S6).

We then investigated whether VCP(DEQ) affected the promoter activities of different genes transcribed by RNA polymerase II. HEK293T cells were transfected with expression vectors for GFP, wtVCP-GFP, or VCP(DEQ)-GFP, along with pHrD-Luc and a well-used vector that expresses luciferase 2. We examined levels of luciferase 2 mRNA by Northern blot and found that luciferase 2 mRNA from all of the tested promoters (*e.g.* those from the cytomegalovirus (CMV) and *EF-1α* genes) was suppressed by the expression of VCP(DEQ)-GFP, but not wtVCP-GFP (Fig. 4*A*, and not shown). Interestingly, this suppression was not fully ameliorated by the addition of butyrate (Fig. 4*A*). Similar decreases in mRNA levels were observed in cells transfected with the Q79 expression vector, but not the Q35 expression vector or empty vector (Fig. 4*B*). Again, this suppression was not fully ameliorated by the addition of butyrate (Fig. 4*B*).

A

600	615	
VINQILTEMDGMSTKK		*Homo sapiens*
VINQILTEMDGMSTKK		*Rattus norvegicus*
VINQILTEMDGMSTKK		*Mus musculus*
VINQILTEMDGMSIKK		*Xenopus laevis*
VINQILTEMDGMGAKK		*Drosophila melanogaster* (ter94)
VINQVLTEMDGMNAKK		*Caenorhabditis elegans* (Cdc48.1)
VLNQLLTEMDGMNAKK		*Arabidopsis thaliana* (Cdc48p)
V-NQLLTEMDGMNAKK		*Saccharomyces cerevisiae* (Cdc48p)

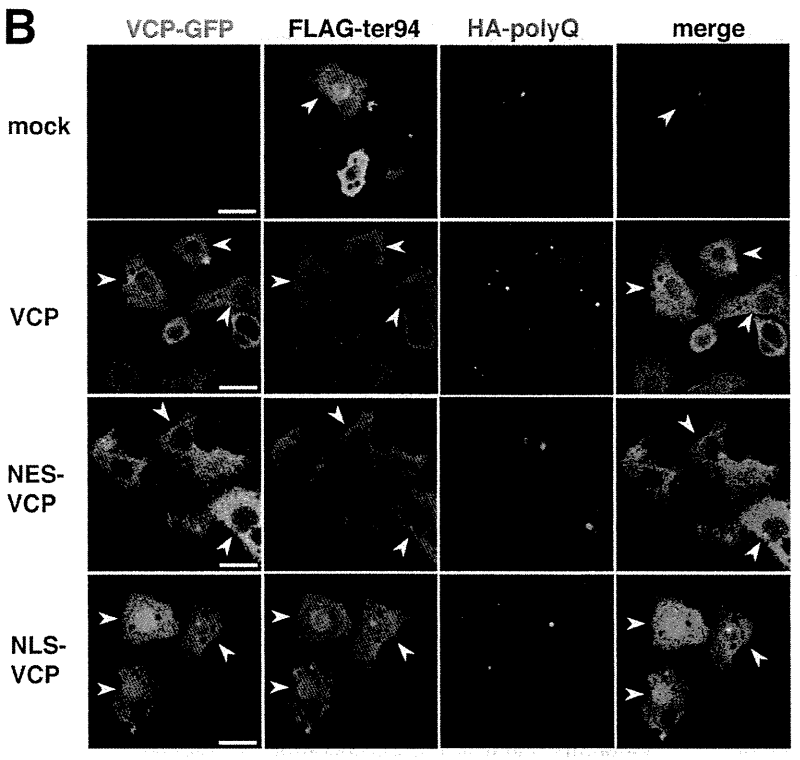

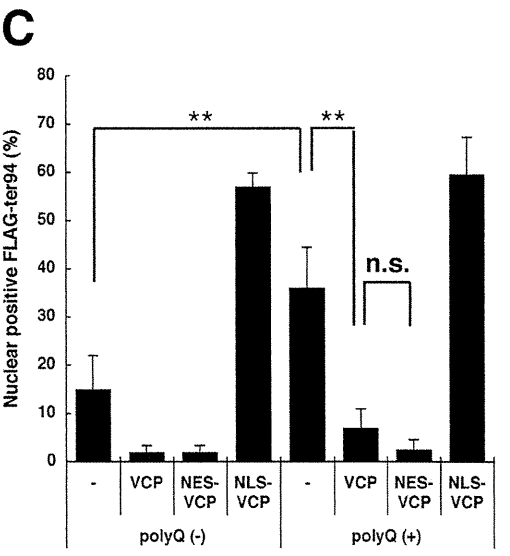

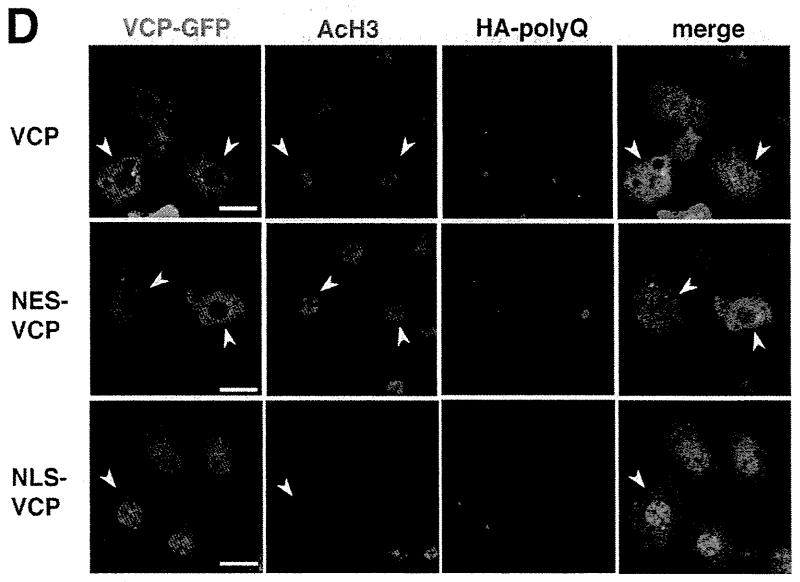

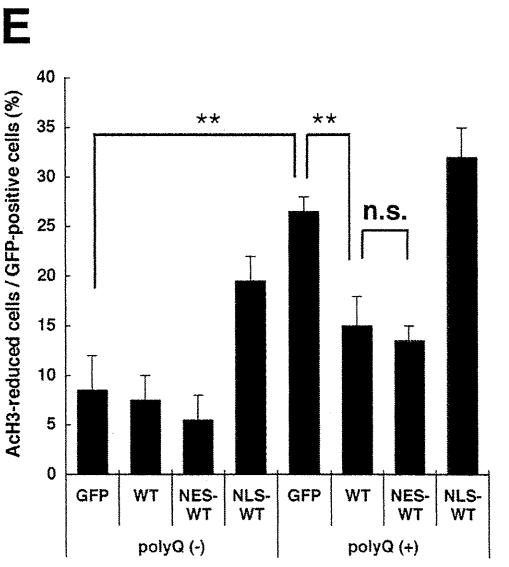

We then performed a similar set of experiments using Tak8 (parental PC12 cells), Tv10 (PC12 cells expressing GFP-tagged wtVCP under the control of the tet-off promoter)(43), DEQ12 (PC12 cells expressing GFP-tagged VCP(DEQ) under the control of the tet-off promoter), and AAA26 cells (PC12 cells expressing GFP-tagged VCP(AAA) under the control of the tet-off promoter) (supplemental Fig. S7). Consistent with the results from the HEK293T cells, luciferase 2 mRNA levels from the CMV promoter were suppressed in DEQ12 cells but not in Tak8, Tv10, or AAA26 cells 3 days after the removal of tetracycline. Again, this suppression was not fully ameliorated by the addition of butyrate (Fig. 4*C*).

The above results indicate that expanded polyglutamine expression induced VCP modifications, which in turn induced suppression of transcription from promoters transcribed by RNA polymerase II but not RNA polymerase I. Thus, we expected *de novo* protein synthesis to be reduced. To investigate this possibility, we examined the levels of *de novo* protein synthesis in Tak8, Tv10, DEQ12, and AAA26 cells by measuring [^{35}S]methionine/cysteine incorporation into newly synthesized proteins. Indeed, we confirmed that *de novo* protein synthesis was significantly decreased in DEQ12 cells, but not in Tv10 or AAA26 cells 5 and 6 days after removal of tetracycline (Fig. 4*D*).

Prevention of Polyglutamine-induced Phenotypes by NES-VCPs in PC12 Cells—We next examined the potential dominant-negative effects of VCP(AAA) on endogenous VCP. In Tak8 cells (parental PC12 cells), tetracycline removal did not affect the intracellular distribution of GFP-tagged wtVCP, VCP(AAA), NES-wtVCP, or NES-VCP(AAA) (Fig. 5*A*). Approximately 20% of cells with GFP signals in the nucleus were expressing wtVCP or VCP(AAA); very few cells with nuclear GFP were expressing NES-wtVCP or NES-VCP(AAA). Similar expression patterns were observed in TQ15 cells (PC12 cells expressing FLAG-Q79 under the control of the tet-off promoter)(40) in the presence of tetracycline. However, tetracycline removal from TQ15 cells, resulting in expression of Q79, induced nuclear translocation of both wtVCP (~80% of cells) and VCP(AAA) (~70% of cells) (Fig. 5*A*). In contrast, only marginal nuclear translocation of NES-wtVCP or NES-VCP(AAA) was observed in TQ15 cells 4 days after removal of tetracycline (Fig. 5*A*). Consistent with these results, overexpression of NES-wtVCP or NES-VCP(AAA) was able to suppress the expanded polyglutamine-induced deacetylation of histone H3 (Fig. 5, *B* and *C*, and not shown), as well as neurite retraction (Fig. 5*D*).

Prevention of Polyglutamine-induced Phenotypes by wtVCP in Drosophila—It is notable that Ser-612 and Thr-613 are changed to Gly and Ala, respectively, in ter94, *Drosophila* VCP (Fig. 6*A*). This suggested the lack of kinases for the phosphorylation of these serine and threonine in *Drosophila*. Given that Ser-612 and Thr-613 of mammalian VCP could not be phosphorylated in *Drosophila*, it was interesting to see whether mammalian VCP was also able to translocate into the nucleus in *Drosophila* cells in the presence of polyglutamine aggregates. We thus examined this possibility using S2R+ cells (41), a *Drosophila* cell line, by expressing FLAG-ter94 with HA-tagged Q92 (Q92). In the absence of Q92 expression, ter94 resided mainly in the cytoplasm. In the presence of Q92 aggregates, ter94 traslocated into the nucleus (Fig. 6*B*, *uppermost panels*). However, wtVCP as well as NES-wtVCP stayed in the cytoplasm, even with co-expression of ter94 in cells with Q92 aggregates (Fig. 6, *B* and *C*). More importantly, not only NES-wtVCP but also wtVCP significantly prevented ter94 nuclear translocation in cells with Q92 aggregates (Fig. 6, *B* and *C*). Consistent with this, in cells expressing wtVCP or NES-wtVCP, acetylation levels of core histones were also significantly recovered even with Q92 aggregates (Fig. 6, *D* and *E*). It is noteworthy that in *Drosophila* S2R+ cells, NLS-VCP itself could induce deacetylation of core histones with its nuclear localization (Fig. 6, *D* and *E*), although this was only marginally observed in mammalian cells (Fig. 3*E*).

We previously showed that overexpression of ter94, *Drosophila* VCP, enhanced polyglutamine-induced eye degenerations (30). It was evident, in contrast, that overexpression of mammalian VCP (wtVCP) in fly eyes clearly suppressed eye degenerations when co-expressed with expanded polyglutamines, without apparently affecting the levels of polyglutamine aggregates (Fig. 7, *A* and *B*). In degenerated eyes, endogenous ter94 located in the nucleus (Fig. 7*C*). In cured eyes, however, overexpressed wtVCP and ter94 predominantly resided in the cytoplasm (Fig. 7*C*), and acetylation levels of core histones were significantly recovered (Fig. 7, *D* and *E*). These results, altogether, indicated that in *Drosophila* cells wtVCP could function in a way similar to NES-wtVCP in mammalian cells, and thus overexpression of wtVCP could mitigate polyglutamine-induced eye degeneration in *Drosophila*. Furthermore expression of VCP(DEQ) itself in fly eyes induced late onset eye degenerations (supplemental Fig. S8). In degenerated eyes, clear reductions in acetylation levels of core histones were observed (supplemental Fig. S8).

DISCUSSION

Several reports have shown that expanded polyglutamine expression decreases the acetylation of core histones such as H3 and H4 (12, 13, 17, 19). We first confirmed this observation in our cell culture model of polyglutamine disease (40). Indeed, the experiments presented here using anti-acetylated H3 (for acetylated Lys-9 and Lys-14) and H4 (for acetylated Lys-5) anti-

FIGURE 6. **Prevention of polyglutamine-induced ter94 nuclear translocation and histone deacetylation by wtVCP in *Drosophila* S2R+ cells.** *A*, amino acid alignment of modified residues in VCP among different species. Lys-614 was widely conserved among different species; Ser-612 and Thr-613 were conserved only in mammals. *B*, immunocytochemical analysis of S2R+ cells transfected with FLAG-ter94 and HA-Q79 (HA-polyQ) with or without GFP-tagged wtVCP(VCP), NES-wtVCP(NES-VCP), and NLS-wtVCP(NLS-VCP). FLAG-ter94 was detected with an anti-FLAG M5 antibody, Q79 with an anti-HA antibody, VCPs with an anti-GFP antibody. Merged images are also shown in the *right panels* with indicated colors. *White arrowheads* show cells with Q79 aggregates. *Bars*, 10 μm. *C*, quantification of immunocytochemical analysis in *B*. At least 200 FLAG-positive cells were imaged randomly and scored. **, $p < 0.01$. *n.s.*, not significant. *D*, immunocytochemical analysis of S2R+ cells transfected with HA-Q79 (*HA-polyQ*) with GFP-tagged wtVCP (*VCP*), NES-wtVCP (*NES-VCP*), and NLS-wtVCP (*NLS-VCP*). Q79 was detected with an anti-HA antibody, acetyl-H3 (AcH3) with an anti-acetylated histone H3 antibody, VCPs with an anti-GFP antibody. Merged images are also shown in the *right panels* with indicated colors. *White arrowheads* indicate cells with Q79 aggregates. *Bars*, 10 μm. *E*, quantification of immunocytochemical analysis in *D*. At least 100 GFP-positive cells were imaged randomly and scored. **, $p < 0.01$; *, $p < 0.05$; *n.s.*, not significant.

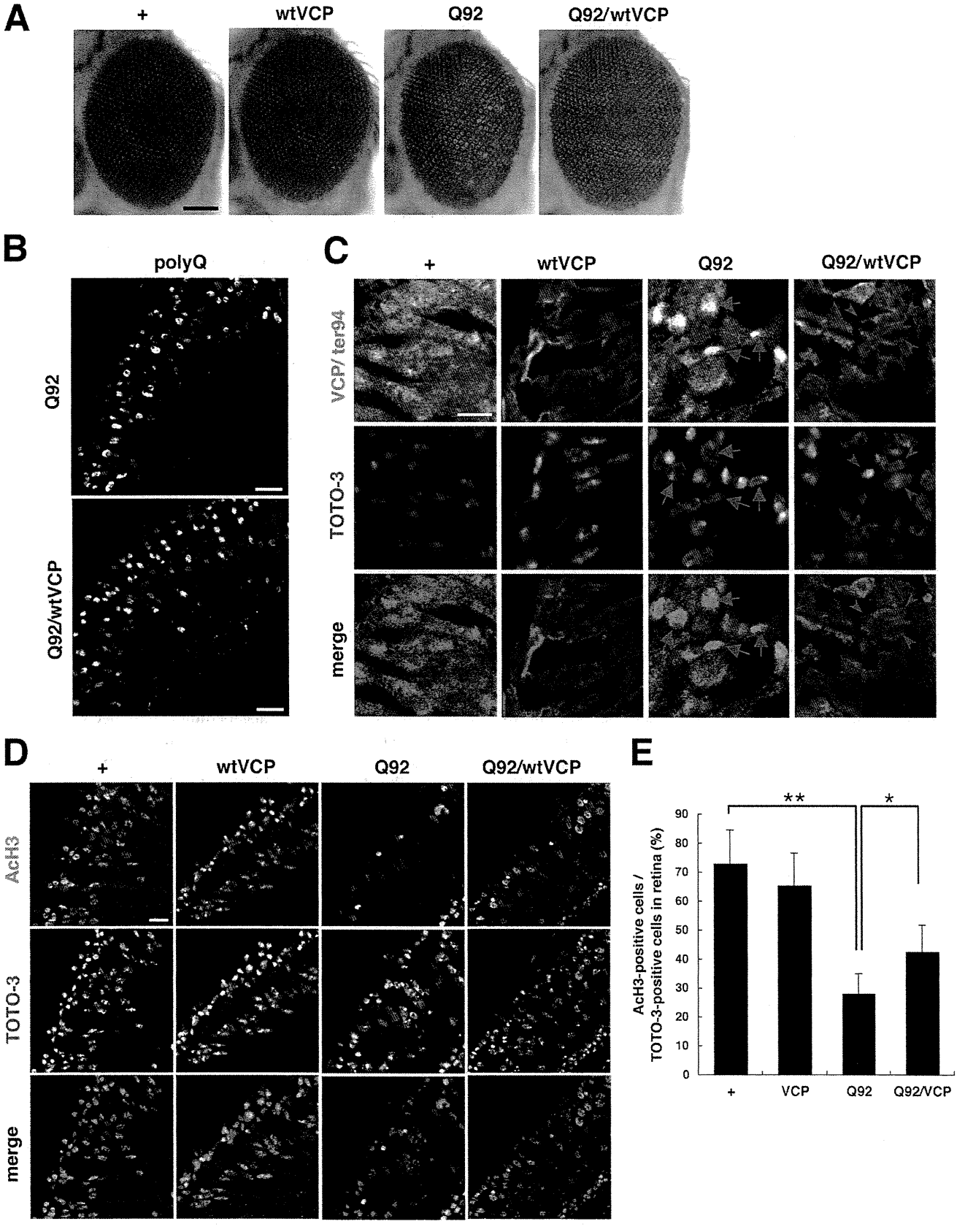

bodies clearly demonstrate a Q79-dependent decrease in H3 and H4 acetylation. In our mouse model of polyglutamine disease (Q64 mice), clear decreases in H4 acetylation were also observed. Addition of butyrate, an inhibitor of HDAC, dramatically recovered or even enhanced the acetylated levels of histones H3 and H4 in PC12 cells, so that cells with or without expanded polyglutamine expression indistinguishable. These observations fit well with the idea that expanded polyglutamine tracts contribute to enhancement of histone deacetylation rather than to diminishment of histone acetylation.

Sequestration of major transcription factors such as CBP within polyglutamine aggregates has been proposed to be the main mechanism underlying transcriptional suppression in aggregate-containing cells (17, 44). Because these transcription factors, either by themselves or by physical interactions, contribute to HAT activation, this putative mechanism would lead to a diminishment of histone acetylation rather than to an enhancement of histone deacetylation, and was in direct contrast with our observations. Furthermore, irrespective of the intracellular localization of polyglutamine aggregates, we observed clear decreases in the acetylated levels of histones H3 and H4. More surprisingly, NES-tagged Q79 could induce stronger histone deacetylation than could NLS-tagged Q79. These observations strongly suggest the existence of a mechanism other than sequestration of transcription factors, in which expanded polyglutamine expression, even in the cytoplasm, leads to H3 and H4 deacetylation, probably via HDAC activation.

In cells expressing expanded polyglutamines, three sequential amino acids in VCP, Ser-612, Thr-613, and Lys-614, were modified by phosphorylation, phosphorylation, and acetylation, respectively. We then examined the biological significance of these modifications by creating and expressing several modification-mimic forms of VCPs, such as VCP(DEQ) and VCP(DEK), in PC12 cells. We also created several control substitutions with alanine, *e.g.* VCP(DEA) and VCP (AAA). Although these substitutions may not perfectly represent modified or non-modified protein configurations, this method has been well-used in elucidating biological functions of the modified or non-modified proteins, respectively, such as kinases, kinase substrates, tubulin, histones etc (45–47).

We found that in more than 95% of cells, exogenously expressed wtVCP stayed in the cytoplasm. In contrast, in more than 60% of transfected cells, exogenously expressed VCP-(DEQ) was translocated to the nucleus, followed by VCP-(DEA)(~50%) and VCP(DEK)(~25%). In accordance with this, FLAG-tagged VCP(DEQ), but not wtVCP, could co-precipitate endogenous importins (data not shown). These results strongly suggest that sequential modifications of Ser-612, Thr-613, and Lys-614 were responsible for the nuclear translocation of VCP. Unexpectedly, these modifications also induced neurite retraction and shrinkage in PC12 cells (~30% of cells), which was also observed in PC12 cells expressing expanded polyglutamine tracts. This atrophic phenotype was not induced by forced expression of NLS-tagged wtVCP in the nucleus or by forced expression of NES-tagged VCP(DEQ) in the cytoplasm. In agreement with these results, forced expression of NLS-tagged VCP(DEQ) in the nucleus further increased the atrophic phenotype in cells (~60% of cells).

The above characteristics of VCP suggest that it might be a mediator of histone deacetylation in response to expanded polyglutamines. Indeed, expression of VCP(DEQ), but not wtVCP or VCP(AAA), induced deacetylation of H3 and H4. More importantly, in mammalian cells NES-wtVCP and NES-VCP(AAA), but not VCP(AAA), inhibited the nuclear translocation of endogenous VCP in cells expressing expanded polyglutamines, and thus could block expanded polyglutamine-induced deacetylation of H3 and H4, as well as the atrophic phenotype. In *Drosophila*, however, wtVCP but not ter94 could prevent ter94 nuclear translocation in a way similar to NES-wtVCP or NES-VCP(AAA) in mammalian cells. Since VCP forms hexameric structure, the observed three sequential modifications of VCP in mammalian cells would not occur so frequently. However, once such modifications occur even in a single or double protomers, the VCP hexamer may be transported into the nucleus. Thus, VCP(AAA) could not suppress the nuclear translocation of the VCP hexamer. In *Drosophila* cells, however, the presence of the unmodified mammalian VCP in the ter94 hexamer did prevent the nuclear translocation of the hexamer even in the presence of polyglutamine aggregates. This might be due to the creation of certain conformations unfavorable for the nuclear translocation of the hexamer by the incorporation of unmodified mammalian VCP. This idea remains to be clarified. In contrast, expression of VCP(DEQ) itself in fly eyes induced eye degenerations, with decreased core histone acetylations. These results demonstrate that VCP is indeed a major mediator of histone deacetylation, as well as a major molecule causative for the atrophic phenotype or eye degenerations in cells expressing expanded polyglutamines. In our mouse model of polyglutamine disease (Q64C mouse), Purkinje cells with nuclear polyglutamine aggregates clearly showed nuclear VCP localization and decrease of acetylation of histone H4. Recently, Reina *et al.* demonstrated that MJD protein/ataxin 3 translocated into the nucleus immediately after the heat shock. In this condition, VCP appeared to stay in the cytoplasm (48). It would also be interesting to see whether histone deacetylation could be observed after the heat shock.

Until now, at least 14 different VCP mutants have been reported to cause IBMPFD. The mutated amino acids include R93C, R95C R95G, R155C, R155H, R155P, G157R, R159H, R159C, R191Q, L198W, A232E, T262A, and N387H (35–39).

FIGURE 7. **Ameliorative effects of wtVCP on polyglutamine-induced eye degeneration and deacetylation of core histones in *Drosophila* eyes.** *A*, light photomicrographs of the compound eyes from 5-day-old flies. Wild-type VCP (*wtVCP*) was expressed alone or together with FLAG-Q92 (*Q92*) in *Drosophila* compound eyes using the GMR promoter. *Bar*, 100 μm. *B–D*, immunohistochemical analysis of tangential head sections from 5-day-old flies. Q92 was detected with an anti-FLAG M5 antibody, acetyl-H3 with an anti-acetylated histone H3 antibody, and VCP/ter94 with an anti-VCP polyclonal antibody. Each section was co-stained with TOTO-3. Merged images are also shown in the *lower panels* with indicated colors. Cells with ter94 dominantly residing in the nucleus are indicated by *red arrows* and with VCP/ter94 dominantly residing outside the nucleus indicated by *red arrowheads* (*C*). *Bars*, 20 μm (*B* and *D*) and 10 μm (*C*). *E*, quantification of immunohistochemical analysis in *D*. More than 200 cells were examined in each sample, and the ratio of nuclei with acetylated histone H3 among TOTO-3-positive nuclei in the retina were counted. **, $p < 0.01$; *, $p < 0.05$.

Except for Thr-262, all other mutations were not observed at serine, threonine, tyrosine, or lysine. Since alanine substitution cannot mimick phosphorylation, all these mutations are not able to be mimicked by post-translational modifications, such as phosphorylations or acetylations. It is notable that all mutations relatively reside at N-terminal portion of VCP. Indeed, these mutant VCPs not only showed enhanced binding abilities to VCP cofactors (*e.g.* Ufd1 and Npl4) and ubiquitinated proteins, but also showed enhanced aggregate-forming activities (Refs. 28, 49).[3] Regarding with these characteristics, we could not observe clear difference between wild-type VCP and VCP(DEQ).[4] Thus, VCP(DEQ) did not appear to be involved in aggregate formation more positively than wild-type VCP or IBMPFD-causing VCPs.

Treatment of cells expressing expanded polyglutamine or VCP(DEQ) by butyrate did result in a recovery from the H3 and H4 deacetylated state to highly acetylated states. However, this treatment only marginally increased transcription from the CMV promoter and several other promoters, such as the EF-1α promoter. These results clearly indicate that the observed transcriptional suppression was mostly mediated by as-yet unknown HDAC inhibitor-insensitive mechanisms.

Based on the results of this study, we propose a novel feedback mechanism linking the accumulation of cytoplasmic misfolded proteins and transcriptional suppression, in which VCP performs an essential role. Intracellular accumulation of abnormal proteins such as expanded polyglutamines induces VCP modification at Ser-612, Thr-613, and Lys-614, which allows VCP to translocate to the nucleus. Following nuclear VCP translocation, general transcription is suppressed by as-yet unknown mechanisms, resulting in the inhibition of *de novo* protein synthesis. This inhibition leads to a decrease in the production of new misfolded proteins, and thus allows to cells to dissolve or degrade the accumulated misfolded proteins by cellular mechanisms such as chaperones, proteasomes, and autophagies. This mechanism would work well when misfolded protein accumulation is transient. However, when misfolded proteins are continuously provided, as in the case of neurodegenerative disorders, inhibition of *de novo* protein synthesis continues for many years or even decades, leading to a gradual decrease in cell mass or shrinkage of affected neurons. Indeed, overexpression of VCP(DEQ) in fly eyes could induce late-onset rough-eye phenotypes. This VCP-mediated feedback mechanism may be a common mechanism underlying neurodegenerative disorders in which there is an intracellular accumulation of abnormal proteins such as polyglutamines, α-synuclein etc.

Acknowledgments—We thank K. Kuroiwa for technical assistance and our laboratory members for valuable discussions. We also thank Drs. T. Kanda and S. Mori (Japan National Institute of Infectious Disease) for pHrD-Luc.

REFERENCES

1. Kaufman, R. J. (2002) *J. Clin. Invest.* **110,** 1389–1398
2. Sidrauski, C., Chapman, R., and Walter, P. (1998) *Trends Cell Biol.* **8,** 245–249
3. Ron, D., and Walter, P. (2007) *Nat. Rev. Mol. Cell Biol.* **8,** 519–529
4. Kakizuka, A. (1998) *Trends Genet.* **14,** 396–402
5. Kobayashi, T., and Kakizuka, A. (2003) *Cytogenet. Genome Res.* **100,** 261–275
6. Neumann, M., Sampathu, D. M., Kwong, L. K., Truax, A. C., Micsenyi, M. C., Chou, T. T., Bruce, J., Schuck, T., Grossman, M., Clark, C. M., McCluskey, L. F., Miller, B. L., Masliah, E., Mackenzie, I. R., Feldman, H., Feiden, W., Kretzschmar, H. A., Trojanowski, J. Q., and Lee, V. M. (2006) *Science* **314,** 130–133
7. Ikeda, H., Yamaguchi, M., Sugai, S., Aze, Y., Narumiya, S., and Kakizuka, A. (1996) *Nat. Genet.* **13,** 196–202
8. Bence, N. F., Sampat, R. M., and Kopito, R. R. (2001) *Science* **292,** 1552–1555
9. Nishitoh, H., Matsuzawa, A., Tobiume, K., Saegusa, K., Takeda, K., Inoue, K., Hori, S., Kakizuka, A., and Ichijo, H. (2002) *Genes Dev.* **16,** 1345–1355
10. Ross, C. A., and Pickart, C. M. (2004) *Trends Cell Biol.* **14,** 703–711
11. Giuliano, P., DeCristofaro, T., Affaitati, A., Pizzulo, G. M., Feliciello, A., Criscuolo, C., DeMichele, G., Filla, A., Avvedimento, E. V., and Varrone, S. (2003) *Hum. Mol. Genet.* **12,** 2301–2309
12. Shimohata, T., Nakajima, T., Yamada, M., Uchida, C., Onodera, O., Naruse, S., Kimura, T., Koide, R., Nozaki, K., Sano, Y., Ishiguro, H., Sakoe, K., Ooshima, T., Sato, A., Ikeuchi, T., Oyake, M., Sato, T., Aoyagi, Y., Hozumi, I., Nagatsu, T., Takiyama, Y., Nishizawa, M., Goto, J., Kanazawa, I., Davidson, I., Tanese, N., Takahashi, H., and Tsuji, S. (2000) *Nat. Genet.* **26,** 29–36
13. Steffan, J. S., Bodai, L., Pallos, J., Poelman, M., McCampbell, A., Apostol, B. L., Kazantsev, A., Schmidt, E., Zhu, Y. Z., Greenwald, M., Kurokawa, R., Housman, D. E., Jackson, G. R., Marsh, J. L., and Thompson, L. M. (2001) *Nature* **413,** 739–743
14. Hassig, C. A., and Schreiber, S. L. (1997) *Curr. Opin. Chem. Biol.* **1,** 300–308
15. Shilatifard, A. (2006) *Annu. Rev. Biochem.* **75,** 243–269
16. Saha, R. N., and Pahan, K. (2006) *Cell Death Differ.* **13,** 539–550
17. Nucifora, F. C., Jr., Sasaki, M., Peters, M. F., Huang, H., Cooper, J. K., Yamada, M., Takahashi, H., Tsuji, S., Troncoso, J., Dawson, V. L., Dawson, T. M., and Ross, C. A. (2001) *Science* **291,** 2423–2428
18. Yu, Z. X., Li, S. H., Nguyen, H. P., and Li, X. J. (2002) *Hum. Mol. Genet.* **11,** 905–914
19. Jiang, H., Nucifora, F. C., Jr., Ross, C. A., and DeFranco, D. B. (2003) *Hum. Mol. Genet.* **12,** 1–12
20. Rouaux, C., Jokic, N., Mbebi, C., Boutillier, S., Loeffler, J. P., and Boutillier, A. L. (2003) *EMBO J.* **22,** 6537–6549
21. Kontopoulos, E., Parvin, J. D., and Feany, M. B. (2006) *Hum. Mol. Genet.* **15,** 3012–3023
22. Rouaux, C., Panteleeva, I., René, F., Gonzalez de Aguilar, J. L., Echaniz-Laguna, A., Dupuis, L., Menger, Y., Boutillier, A. L., and Loeffler, J. P. (2007) *J. Neurosci.* **27,** 5535–5545
23. Whiteheart, S. W., and Matveeva, E. A. (2004) *J. Struct. Biol.* **146,** 32–43
24. Braun, R. J., and Zischka, H. (2008) *Biochim. Biophys. Acta* **1783,** 1418–1435
25. Hirabayashi, M., Inoue, K., Tanaka, K., Nakadate, K., Ohsawa, Y., Kamei, Y., Popiel, A. H., Sinohara, A., Iwamatsu, A., Kimura, Y., Uchiyama, Y., Hori, S., and Kakizuka, A. (2001) *Cell Death Differ.* **8,** 977–984
26. Mizuno, Y., Hori, S., Kakizuka, A., and Okamoto, K. (2003) *Neurosci. Lett.* **343,** 77–80
27. Ishigaki, S., Hishikawa, N., Niwa, J., Iemura, S., Natsume, T., Hori, S., Kakizuka, A., Tanaka, K., and Sobue, G. (2004) *J. Biol. Chem.* **279,** 51376–51385
28. Kakizuka, A. (2008) *Biochem. Soc. Trans.* **36,** 105–108
29. Kobayashi, T., Manno, A., and Kakizuka, A. (2007) *Genes Cells* **12,** 889–901
30. Higashiyama, H., Hirose, F., Yamaguchi, M., Inoue, Y. H., Fujikake, N., Matsukage, A., and Kakizuka, A. (2002) *Cell Death Differ.* **9,** 264–273
31. Klein, J. B., Barati, M. T., Wu, R., Gozal, D., Sachleben, L. R., Jr., Kausar, H., Trent, J. O., Gozal, E., and Rane, M. J. (2005) *J. Biol. Chem.* **280,** 31870–31881
32. Livingstone, M., Ruan, H., Weiner, J., Clauser, K. R., Strack, P., Jin, S.,

[3] A. Manno and A. Kakizuka, unpublished observations.
[4] K. Yasuda and A. Kakizuka, unpublished observations.

Williams, A., Greulich, H., Gardner, J., Venere, M., Mochan, T. A., DiTullio, R. A., Jr., Moravcevic, K., Gorgoulis, V. G., Burkhardt, A., and Halazonetis, T. D. (2005) *Cancer Res.* **65,** 7533–7540
33. Noguchi, M., Takata, T., Kimura, Y., Manno, A., Murakami, K., Koike, M., Ohizumi, H., Hori, S., and Kakizuka, A. (2005) *J. Biol. Chem.* **280,** 41332–41341
34. Mori-Konya, C., Kato, N., Maeda, R., Yasuda, K., Higashimae, N., Noguchi, M., Koike, M., Kimura, Y., Ohizumi, H., Hori, S., and Kakizuka, A. (2009) *Genes Cells* **14,** 483–497
35. Watts, G. D., Wymer, J., Kovach, M. J., Mehta, S. G., Mumm, S., Darvish, D., Pestronk, A., Whyte, M. P., and Kimonis, V. E. (2004) *Nat. Genet.* **36,** 377–381
36. Haubenberger, D., Bittner, R. E., Rauch-Shorny, S., Zimprich, F., Mannhalter, C., Wagner, L., Mineva, I., Vass, K., Auff, E., and Zimprich, A. (2005) *Neurology* **65,** 1304–1305
37. Forman, M. S., Mackenzie, I. R., Cairns, N. J., Swanson, E., Boyer, P. J., Drachman, D. A., Jhaveri, B. S., Karlawish, J. H., Pestronk, A., Smith, T. W., Tu, P. H., Watts, G. D., Markesbery, W. R., Smith, C. D., and Kimonis, V. E. (2006) *J. Neuropathol. Exp. Neurol.* **65,** 571–581
38. Kimonis, V. E., Fulchiero, E., Vesa, J., and Watts, G. (2008) *Biochim. Biophys. Acta* **1782,** 744–748
39. Djamshidian, A., Schaefer, J., Haubenberger, D., Stogmann, E., Zimprich, F., Auff, E., and Zimprich, A. (2009) *Muscle Nerve* **39,** 389–391
40. Yasuda, S., Inoue, K., Hirabayashi, M., Higashiyama, H., Yamamoto, Y., Fuyuhiro, H., Komure, O., Tanaka, F., Sobue, G., Tsuchiya, K., Hamada, K., Sasaki, H., Takeda, K., Ichijo, H., and Kakizuka, A. (1999) *Genes Cells* **4,** 743–756
41. Yanagawa, S., Lee, J. S., and Ishimoto, A. (1998) *J. Biol. Chem.* **273,** 32353–32359
42. Mori, S., Ozaki, S., Yasugi, T., Yoshikawa, H., Taketani, Y., and Kanda, T. (2006) *Mol. Cell. Biochem.* **288,** 47–57
43. Kobayashi, T., Tanaka, K., Inoue, K., and Kakizuka, A. (2002) *J. Biol. Chem.* **277,** 47358–47365
44. Schaffar, G., Breuer, P., Boteva, R., Behrends, C., Tzvetkov, N., Strippel, N., Sakahira, H., Siegers, K., Hayer-Hartl, M., and Hartl, F. U. (2004) *Mol. Cell* **15,** 95–105
45. Holmberg, C. I., Tran, S. E., Eriksson, J. E., and Sistonen, L. (2002) *Trends Biochem. Sci.* **27,** 619–627
46. Gaertig, J., and Wloga, D. (2008) *Curr. Top. Dev. Biol.* **85,** 83–113
47. Edmondson, D. G., Davie, J. K., Zhou, J., Mirnikjoo, B., Tatchell, K., and Dent, S. Y. (2002) *J. Biol. Chem.* **277,** 29496–29502
48. Reina, C. P., Zhong, X., and Pittman, R. N. (2010) *Hum. Mol. Genet.* **19,** 235–249
49. Ju, J. S., Miller, S. E., Hanson, P. I., and Weihl, C. C. (2008) *J. Biol. Chem.* **283,** 30289–30299
50. Trottier, Y., Luts, Y., Stevanin, G., Imbert, G., Devys, D., Cancel, G., Saudou, F., Weber, C., David, G., Tora, L., Agid, Y., Brice, A., and Mandel, J. L. (1995) *Nature* **378,** 403–406

Genes to Cells

Enhanced ATPase activities as a primary defect of mutant valosin-containing proteins that cause inclusion body myopathy associated with Paget disease of bone and frontotemporal dementia

Atsushi Manno[1,2], Masakatsu Noguchi[1,2], Junpei Fukushi[1,2], Yasuhiro Motohashi[1,2] and Akira Kakizuka[1,2]*

[1]*Laboratory of Functional Biology, Kyoto University Graduate School of Biostudies, Kyoto 606-8501, Japan*
[2]*SORST, Japan Science and Technology Agency*

Valosin-containing protein (VCP) has been shown to colocalize with abnormal protein aggregates, such as nuclear inclusions of Huntington disease and Machado-Joseph disease, Lewy bodies in Parkinson disease. Several mis-sense mutations in the human *VCP* gene have been identified in patients suffering inclusion body myopathy associated with Paget disease of bone and frontotemporal dementia (IBMPFD). Recently, we have shown that VCP possesses both aggregate-forming and aggregate-clearing activities. Here, we showed that in cells treated with proteasome inhibitors VCP first appeared as several small aggregates throughout the cells; and then, these small aggregates gathered together into a single big aggregate. Subcellular localization and ATPase activity of VCP clearly influenced the localization of the aggregates. Furthermore, all tested IBMPFD-causing mutant VCPs, possessed elevated ATPase activities and enhanced aggregate-forming activities in cultured cells. In *Drosophila*, these mutants and VCP(T761E), a super active VCP, did not appear to spontaneously induce eye degeneration, but worsened the phenotype when co-expressed with polyglutamines. Unexpectedly, these VCPs did not apparently change sizes and the amounts of polyglutamine aggregates in *Drosophila* eyes. Elevated ATPase activities, thus, may be a hidden primary defect causing IBMPFD pathological phenotypes, which would be revealed when abnormal proteins are accumulated, as typically observed in aging.

Introduction

VCP belongs to the AAA (ATPase associated with diverse cellular activities) proteins, forms a homohexameric structure and consists of the N-terminal domain (N domain), two ATPase domains (D1 and D2 domains) and the C-terminal domain (Zhang *et al.* 2000; Dalal & Hanson 2001; Brunger & DeLaBarre 2003; Wang *et al.* 2004). VCP is one of the most abundant and ubiquitous intracellular proteins (Dalal & Hanson 2001). It has been shown that VCP is involved in diverse cellular activities, including proteasome-mediated protein degradation, endoplasmic reticulum (ER)-associated degradation (ERAD), membrane fusions and mitosis (Wang *et al.* 2004). In performing different functions, VCP has been proposed to differentially use its partners, e.g. Ufd1, Npl4, p47 (Dreveny *et al.* 2004). VCP has been also shown to be modified at many amino acid residues throughout the protein via oxidation, phosphorylation and acetylation (Noguchi *et al.* 2005; Mori-Konya *et al.* 2009; Koike *et al.* 2010). Previously, we have identified VCP as a binding partner of the Machado-Joseph disease (MJD) protein with expanded polyglutamines, which causes MJD, the most common inherited spinocerebellar ataxia (Kawaguchi *et al.* 1994; Hirabayashi *et al.* 2001). We have also identified *ter94*, *Drosophila* homologue of VCP, as a modifier of expanded polyglutamine-induced eye degeneration by genetic screening using our *Drosophila* polyglutamine disease models (Higashiyama *et al.* 2002). Interestingly,

Communicated by: Eisuke Nishida
**Correspondence*: kakizuka@lif.kyoto-u.ac.jp

DOI: 10.1111/j.1365-2443.2010.01428.x

we have shown that VCP colocalized with abnormal protein aggregates or ubiquitin-positive inclusion bodies in neurons suffering from several neurodegenerative disorders including not only MJD but also Huntington disease, Parkinson disease, motor neuron disease and so on (Hirabayashi *et al.* 2001; Mizuno *et al.* 2003; Ishigaki *et al.* 2004). Under the proteasome inhibition and/or the accumulation of ubiquitin-positive proteins, small aggregates are first formed in the cytoplasm, and then they are transported to the microtubule organizing center near the nucleus (Johnston *et al.* 1998; García-Mata *et al.* 1999). The resultant ubiquitin-positive structure is called the aggresome (Johnston *et al.* 1998). The transport has been proposed to occur along the microtubules by dynein/dynactin motor proteins and HDAC6 (Johnston *et al.* 2002; Kawaguchi *et al.* 2003). The aggresome is also surrounded by vimentin, an intermediate filament protein, and thus ubiquitin and vimentin stainings are well used to elucidate the position of aggresome in histochemical studies. VCP immunostaining was also observed in aggresomes induced by proteasome inhibition and in polyglutamine aggregates in cells expressing expanded polyglutamines (Hirabayashi *et al.* 2001). However, the significance of such colocalization remains to be elucidated. Recently, we have demonstrated that VCP is involved in the formation and/or clearance of abnormal protein aggregates and that it is also involved in the re-solubilization and re-activation of heat-denatured proteins from insoluble aggregates (Kobayashi *et al.* 2007). Hence, we have proposed that VCP functions not only as an aggregate-formase but also as an aggregate-unfoldase (Kobayashi *et al.* 2007).

Inclusion body myopathy associated with Paget disease of bone and frontotemporal dementia (IBMPFD) is a rare, complex, late-onset and ultimately lethal disorder with the autosomal dominant inheritance (OMIM 605382) (Kimonis *et al.* 2000; Watts *et al.* 2004). The most common manifestation is adult-onset muscle weakness with myopathy (80–90% of affected individuals). Paget disease of bone (PDB) and frontotemporal dementia (FTD) occur less frequently than muscle myopathy (43–57%; PDB, 27–37%; FTD) (Kimonis *et al.* 2000, 2008; Kovach *et al.* 2001; Kimonis & Watts 2005). Several groups have reported that 7 mis-sense mutations in the gene encoding VCP were identified among the patients with IBMPFD (277C → T, 283C → G, 463C → T, 464G → A, 464G → C, 476G → A, 572G → A and 695C → A, resulting in the amino acid substitutions R93C, R95G, R155C, R155H, R155P, R159H, R191Q and A232E) (Watts *et al.* 2004; Haubenberger *et al.* 2005; Hübbers *et al.* 2007). Furthermore, novel mutations in VCP (R95C, G157R, R159C, L198W, T262A and N387H) have also been reported (Forman *et al.* 2006; Watts *et al.* 2007; Djamshidian *et al.* 2009; Weihl *et al.* 2009). Among 10 amino acid residues mutated in IBMPFD, 7 are conserved between *Drosophila* and human beings (R155, R159, R191, L198, A232, T262 and N387 are conserved, but not R93, R95 or G157) (Mori-Konya *et al.* 2009). It is notable that Arg93 is changed to Cys in *Drosophila*. In skeletal muscles and in neurons of the central nervous system of patients with IBMPFD, VCP-positive aggregates or VCP-rimmed vacuoles were observed (Watts *et al.* 2004; Schröder *et al.* 2005). Recently, it has been reported that IBMPFD-associated VCP mutants disrupt ERAD (Weihl *et al.* 2006), impair aggresome formation (Ju *et al.* 2008) as well as autophagy (Ju *et al.* 2009). However, pathogenic mechanisms underlying IBMPFD are still controversial and remain unclear.

In this study, we demonstrate that all tested IBMPFD-associated VCP mutants possess elevated ATPase activities as well as enhanced aggregate-forming activities together with cofactor-binding abilities especially on Ufd1 and Npl4 in mammalian cells, which apparently enhances their binding abilities to ubiquitinated proteins. Furthermore, VCP mutants of higher ATPase activities worsened the phenotypes when co-expressed with polyglutamines in *Drosophila* eyes, even without apparently affecting aggregates. These observations suggest that constitutively elevated ATPase activities of VCP are primary abnormalities causing IBMPFD.

Results

VCP in abnormal protein aggregate formation

In order to define the way as to how VCP involves in protein aggregate formation, we transfected HEK293 cells with expression vectors for VCP-GFP and FLAG-Q35 (Q35) or -Q79 (Q79), which encodes FLAG-tagged 35 or 79 repeats of glutamine residues, respectively, and examined their colocalization. One day after transfection, we found that VCP-GFP colocalized with small Q79 aggregates, which appeared as several dots throughout the cells (Fig. 1A, middle panels). Two days after transfection, most cells had one big aggregate, and this aggregate was labeled with GFP signals (Fig. 1A, lower panels). To examine the entire processes more precisely, we traced GFP

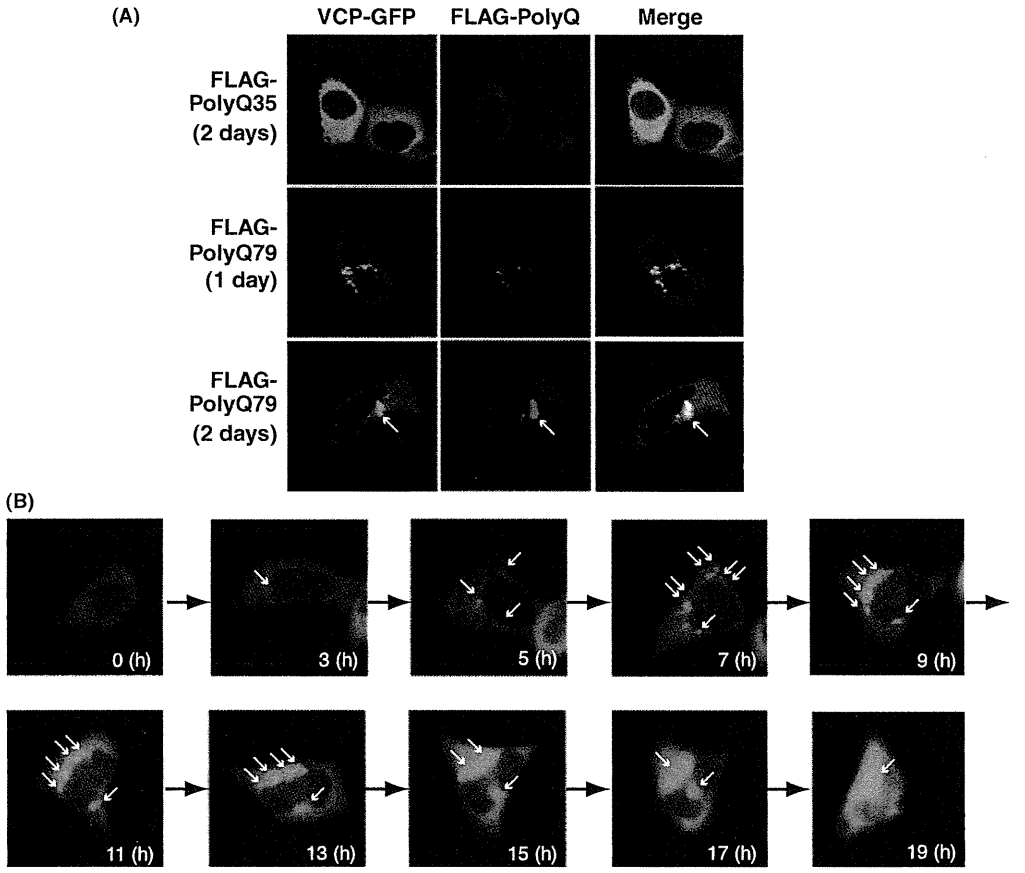

Figure 1 Localization of valosin-containing protein (VCP) in protein aggregates in cultured cells. (A) Localization of VCP and polyglutamine aggregates in HEK293 cells co-expressing VCP-GFP and FLAG-Q35 or -Q79 for 1 or 2 days. VCP (green signals), and Q35 or Q79 (red signals) were visualized via fluorescence microscopy. (B) After expression of VCP-GFP and treatment with 1 μM MG132 (time 0 h), HEK293 cells were examined under time-lapse fluorescence microscopy. Several small protein aggregates were observed in the cytoplasm after 3–7 h; and then, these small aggregates were gathered to a single large aggregate after 9–19 h. White arrows indicate positions of aggregates (A) and (B).

signals in a HEK293 cell expressing VCP-GFP after treatment with MG132 (a proteasome inhibitor), which is known to create the aggresome in the cytoplasm (Johnston *et al.* 1998). Before treatment with MG132, VCP-GFP was distributed diffusely throughout the cytoplasm in the cell, but approximately 3–6 h after the treatment, GFP signals appeared as small dots in several different portions of the cell. Then, after 9–19 h, these GFP-positive small aggregates moved to a single big aggregate, which is generally called an aggresome (Johnston *et al.* 1998) (Fig. 1B, Video S1 in Supplementary materials.).

These results suggested that VCP may function as a carrier of abnormal proteins for collecting them into the aggresome. If so, VCP localization may affect the localizations of protein aggregates. In order to test this, we expressed Q79 together with VCP-GFP, NES-VCP-GFP or NLS-VCP-GFP in HEK293 cells and examined the localizations of the aggregates. Among the GFP-positive cells, less than 10% of the cells contained Q79 aggregates in the nucleus in HEK293 cells expressing VCP-GFP or NES-VCP-GFP, in which GFP signals were observed mostly in the cytoplasm (Fig. 2A,B). On the other hand, nearly 50% of cells contained Q79 aggregates in the nucleus of HEK293 cells expressing NLS-VCP-GFP, where GFP signals were observed mostly in the nucleus (Fig. 2A,B). Interestingly, when we expressed NLS-tagged VCP(K524A), an ATPase activity-deficient VCP mutant (Hirabayashi *et al.* 2001; Kobayashi *et al.*

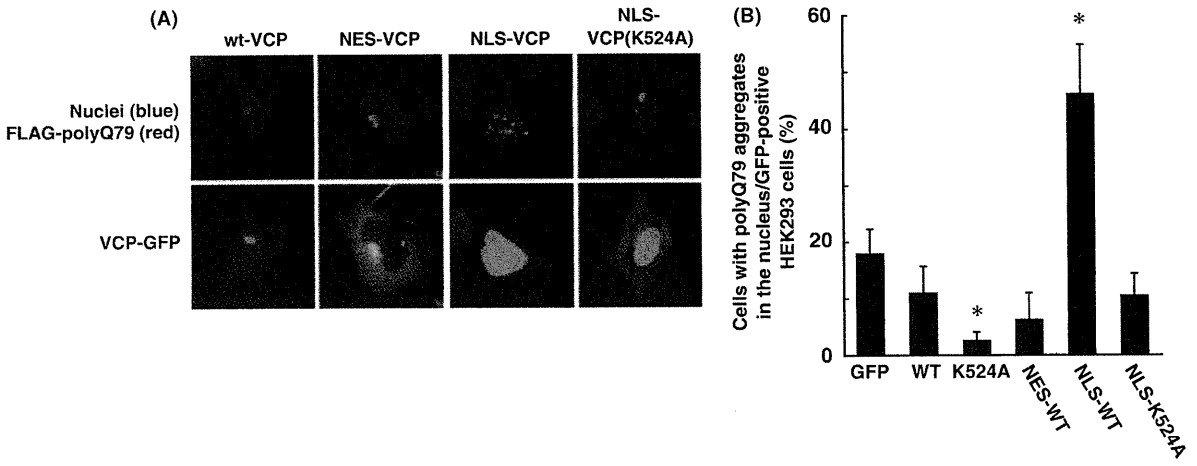

Figure 2 Effects of valosin-containing protein (VCP) on the polyglutamine aggregate formation. (A) HEK293 cells were transfected with wt-VCP-GFP, NES-wt-VCP-GFP, NLS-wt-VCP-GFP or NLS-VCP(K524A)-GFP, together with FLAG-Q79. Two days after transfection, cells were processed for immunochemical analysis. VCP (green signals), Q79 (red signals) and nuclei (blue signals) were visualized via fluorescence microscopy. Note that in cells expressing NES-VCP, a big single polyQ aggregate was observed in microtubule organizing center near the nucleus. (B) The numbers of cells with polyglutamine aggregates in the nucleus and GFP-positive cells were counted in five different fields in the condition described in (A), and percentages of cells with polyglutamine aggregates in the nucleus among GFP-positive cells are shown. Mean values of five independent fields are indicated. Error bars represent standard deviations. Statistical analysis was performed by Student's *t*-test (*$P < 0.01$ vs. WT).

2002), Q79 aggregates were observed mostly in the cytoplasm but not in the nucleus in the cells (Fig. 2A,B), although the aggregates were less frequently formed. These results suggest that the VCP is able to transport abnormal proteins, probably functioning as a carrier, and that its ATPase activities are necessary for this performance.

Involvement of VCP cofactors in aggregate formation

We then investigated the role of VCP cofactors on abnormal protein aggregate formation using the RNAi technique. We examined the efficiency of various siRNAs on the polyglutamine aggregate formation in HEK293 cells (Fig. 3). In Western blotting, we observed that VCP siRNA decreased expression levels of not only VCP but also Npl4 and Ufd1 (Fig. 3A). p47 siRNA specifically reduced p47 expression levels (Fig. 3A), whereas Npl4 siRNA almost completely depleted expression levels of both Npl4 and Ufd1 (Fig. 3A). Likewise, Ufd1 siRNA induced a strong depletion of Ufd1 as well as a weak depletion of Npl4 (Fig. 3A). Previously, it has been reported that Npl4 siRNA decreased Ufd1 protein levels and that Ufd1 siRNA or Npl4 siRNA decreased VCP-Ufd1-Npl4 complex by approximately 90% (Nowis *et al.* 2006). These data and our data did not match perfectly, but as a whole, suggest that protein levels of VCP, Npl4 and Ufd1 were affected by each other. We observed that not only the decrease in VCP, but also the decrease in Npl4 and Ufd1 inhibited Q79 aggregate formation by immunochemical analysis in HEK293 cells (Fig. 3B,C). In contrast, decrease in p47 did not apparently affect the aggregate formation (Fig. 3B,C).

Enhancement of aggregate-forming and ATPase activities in IBMPFD-VCPs

Recently, we have proposed that VCP functions as both an aggregate-formase and aggregate-unfoldase (Kobayashi *et al.* 2007). The results earlier suggested that VCP functions as a carrier of abnormal proteins into aggregates. These results led to the possibility that IBMPFD-causing VCP mutants cause the acceleration of abnormal protein aggregate formation. To address this possibility, we examined the effects of the expression of IBMPFD-causing VCP mutants (IBMPFD-VCPs) on forming abnormal protein aggregates induced by proteasome inhibition or expanded polyglutamine expression. By treatment with proteasome inhibitors, we found significant increase in cell populations having aggregated GFP signals by expressing all tested GFP-tagged IBMPFD-

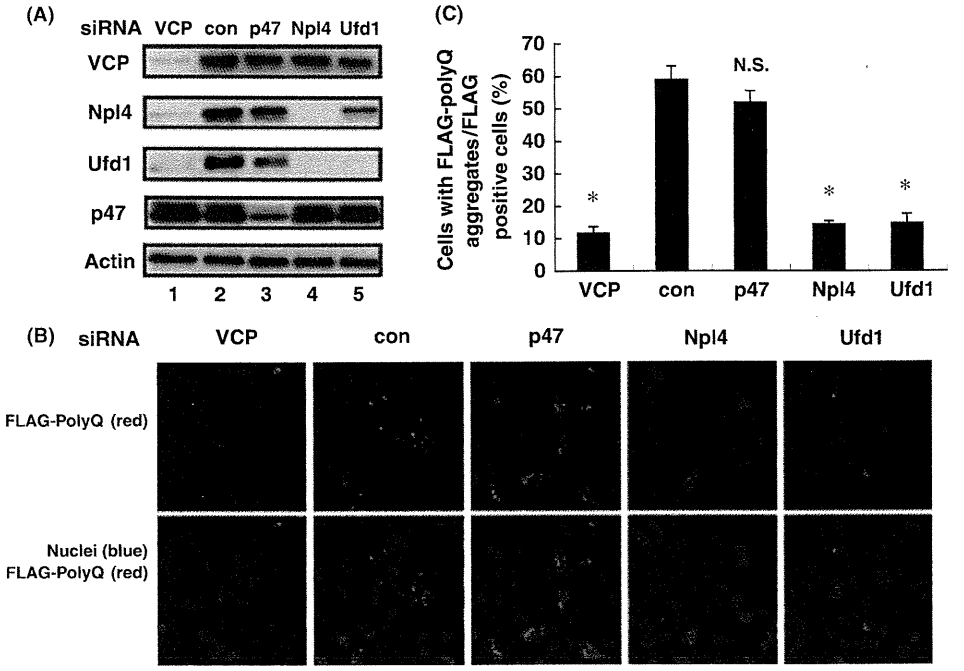

Figure 3 Effects of valosin-containing protein (VCP) cofactors on the polyglutamine aggregate formation. (A) Effects of VCP cofactors depletion by siRNA in HEK293 cells. HEK293 cells were transfected with VCP siRNA (ncds), control siRNA, p47 siRNA (1477), Npl4 siRNA (679) and Ufd1 siRNA (216). Expression levels of VCP, Npl4, Ufd1, p47 and actin, as a loading control, were detected by Western blot analysis. (B) Formation of polyglutamine aggregates in cells expressing both FLAG-Q79 and VCP siRNA (ncds), control siRNA, p47 siRNA (1477), Npl4 siRNA (679) and Ufd1 siRNA (216). The cells described in (A) were visualized by fluorescence microscopy, and Q79 (red signals) and the nucleus (blue signals) were visualized. (C) Effects of the knockdown of VCP cofactors on the polyglutamine aggregate formation. The numbers of cells with polyglutamine aggregates and FLAG-positive cells were counted in five different fields in condition described in (A), and the percentages of cells with polyglutamine aggregates among FLAG-positive cells are shown. Mean values of five independent fields are indicated. Error bars represent standard deviations. Statistical analysis was performed by Student's *t*-test (*$P < 0.01$; N.S., not significant vs. control siRNA).

VCPs when compared to expressing GFP-tagged wt-VCP (Fig. 4A). We also transfected HEK293 cells with GFP-tagged VCP(K524A) or VCP(K251A), ATPase activity-deficient VCP mutants (Hirabayashi *et al.* 2001; Kobayashi *et al.* 2002). By adding proteasome inhibitors on cells expressing VCP(K251A)-GFP or VCP(K524A)-GFP, cell populations having aggregated GFP signals were significantly decreased when compared with cells expressing wt-VCP (Fig. 4A). Regarding with polyglutamine aggregates, we also observed significant increases in cell populations with aggregated GFP signals in cells expressing most of IBMPFD-VCPs and significant decreases in cells expressing ATPase activity-deficient mutants (Fig. 4B). Collectively, these data provided the evidence that formation of abnormal protein aggregates is enhanced in cells expressing IBMPFD-VCPs when compared with wt-VCP, as similar results have been published (Weihl *et al.* 2006).

We also noticed that enhancement of abnormal protein aggregate formation in cells expressing VCP(T761E), a super active VCP in HEK293 cells (Fig. 4A,B), which has more than twice as strong ATPase activity than wt-VCP (Mori-Konya *et al.* 2009). From these results, we hypothesized that ATPase activities of IBMPFD-VCPs would be higher than that of wt-VCP. We thus measured their ATPase activities and found that all tested IBMPFD-VCPs showed significantly higher ATPase activities, when compared with that of wt-VCP in two different assays (Fig. 4C,D).

We next investigated the binding abilities of IBMPFD-VCPs to VCP cofactors. We transfected HEK293 cells with FLAG-tagged wt-VCP, VCP

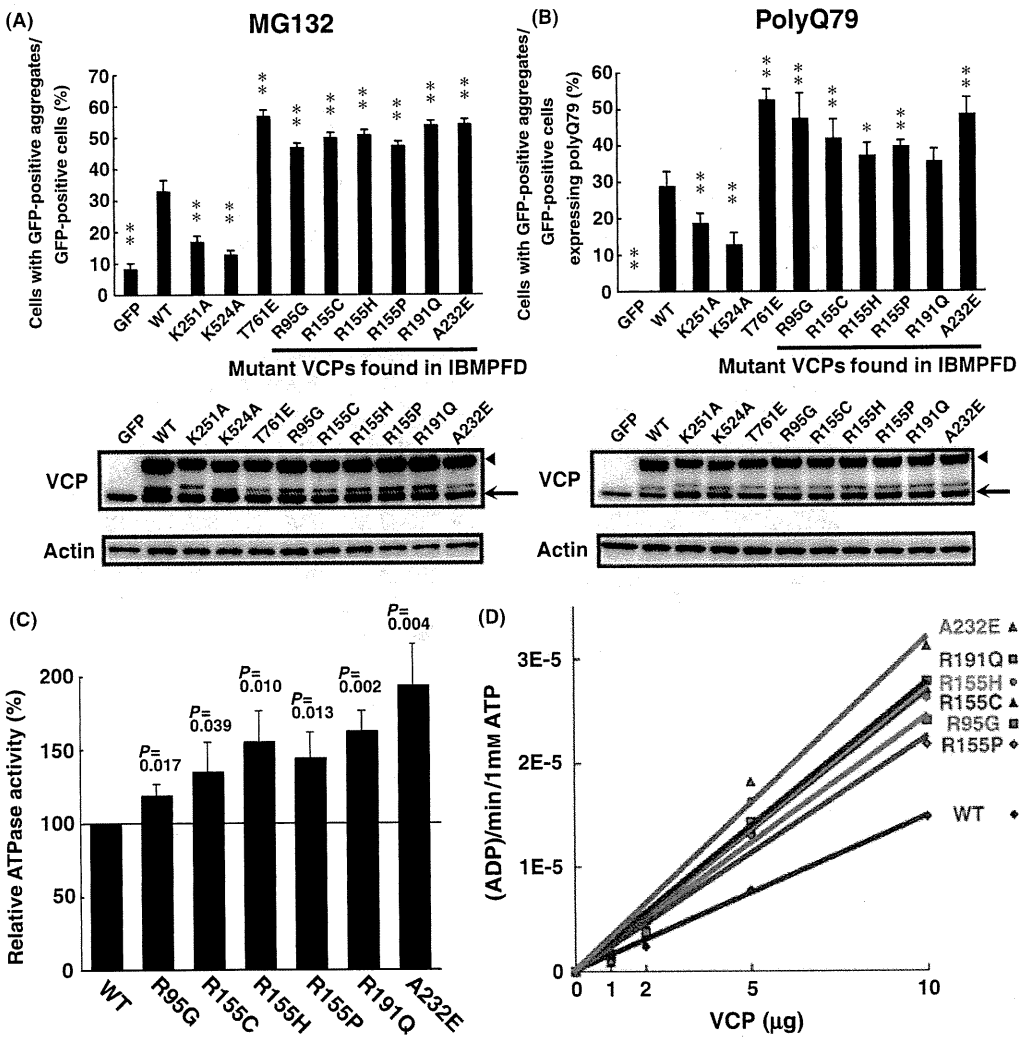

Figure 4 Enhanced aggregate-forming activities and ATPase activities in IBMPFD-VCPs. (A) Enhanced activities for MG132-induced aggregate formation in IBMPFD-VCPs. HEK293 cells were transfected with an expression plasmid for GFP or GFP-tagged VCPs. Twelve hours after transfection, cells were treated with 0.3 μM MG132 for 24 h. The number of cells with GFP-positive aggregates and GFP-positive cells was counted in five different fields. The percentages of cells with aggregates among GFP-positive cells are shown in the upper graph. Expression levels of various VCP-GFPs (VCP) and actin (actin) as a loading control are indicated in the lower panels. Arrowhead indicates bands of VCP-GFP, and arrow indicates bands of endogenous VCP. (B) Enhanced activities for polyglutamine aggregate formation in IBMPFD-VCPs. HEK293 cells were transfected with both an expression plasmid for GFP or GFP-tagged VCPs and an expression plasmid for FLAG-Q79. One day after transfection, the numbers of cells with GFP-positive aggregates and GFP-positive cells expressing FLAG-Q79 were counted in five different fields. The percentages of cells with GFP-positive aggregates among GFP-positive cells expressing FLAG-Q79 are shown in the upper graph. Expression levels of various VCP-GFPs (VCP) and actin (actin) as a loading control are indicated in the lower panels. Arrowhead indicates bands of VCP-GFP, and arrow indicates bands of endogenous VCP. Mean values of five independent fields are indicated. The error bars represent standard deviations. Statistical significance was calculated by Tukey's test (**$P < 0.01$, *$P < 0.05$ vs. WT, $n = 5$) (A) and (B). (C) and (D) Up-regulation of ATPase activities in IBMPFD-VCPs. ATPase activities of recombinant VCPs purified by HEK293 free style cells were compared. Their ATPase activities were measured using both the molybdate assay (C) and the NADH-coupled assay (D). See Experimental procedures in detail. Mean values of triplicate experiments are shown. Error bars represent standard deviations. *P*-values analyzed by Student's *t*-test are shown above the columns (C). IBMPFD, inclusion body myopathy associated with Paget disease of bone and frontotemporal dementia; VCP, valosin-containing protein.